Analysis of Earthquake Motions Recorded During the Kocaeli Earthquake, Turkey 1999

B. Teymur, S.P.G. Madabhushi and D.E.Newland

CUED/D-Soils/TR312 (2000)

Abstract

The Marmara region of Turkey was shaken by an earthquake with a magnitude of 7.4 and epicentre in Golcuk on August 17, 1999. During the main shock, 17000 people died and 45000 were injured. Structural damage of various degrees occurred in Adapazari, Golcuk, Yalova, Izmit and Istanbul. Damage due to liquefaction, surface subsidence, fault rupture, ground shaking and slope instability were also observed. In this technical report the acceleration traces recorded at various locations are closely inspected using power spectrum analysis and harmonic wavelet analysis.

A new signal analysis technique based on harmonic wavelet analysis was used to look at the earthquake induced accelerations. The superiority of this method when dealing with non-stationary signals like earthquakes is that one can plot the signal in a time-frequency space enabling the energy distribution in the signal to be observed. It is quicker to recognise many characteristics of the signal with the wavelet analysis such as the frequency-time and acceleration-time. Frequency-time information is more useful in understanding the earthquake motion than the traditional Discrete Fast Fourier techniques.

The harmonic wavelet method was applied to some of the signals obtained from the Kocaeli Earthquake, 1999. YPT, ARC, CNA and BUR signals were chosen due to their increasing distance from the epicentre. The change of earthquake characteristics with the distance to the epicentre was investigated. As one moves away from the epicentre, the energy of the earthquake decreases. Notably in this earthquake, the attenuation of the peak accelerations in the EW direction was lower than in the NS direction strongly supporting the unzipping of the fault along the EW direction.

Abstract

The Marmara region of Turkey was shaken by an earthquake with a magnitude of 7.4 and epicentre in Golcuk on August 17, 1999. During the main shock, 17000 people died and 45000 were injured. Structural damage of various degrees occurred in Adapazari, Golcuk, Yalova, Izmit and Istanbul. Damage due to liquefaction, surface subsidence, fault rupture, ground shaking and slope instability were also observed. In this technical report the acceleration traces recorded at various locations are closely inspected using power spectrum analysis and harmonic wavelet analysis.

A new signal analysis technique based on harmonic wavelet analysis was used to look at the earthquake induced accelerations. The superiority of this method when dealing with non-stationary signals like earthquakes is that one can plot the signal in a time-frequency space enabling the energy distribution in the signal to be observed. It is quicker to recognise many characteristics of the signal with the wavelet analysis such as the frequency-time and acceleration-time. Frequency-time information is more useful in understanding the earthquake motion than the traditional Discrete Fast Fourier techniques.

The harmonic wavelet method was applied to some of the signals obtained from the Kocaeli Earthquake, 1999. YPT, ARC, CNA and BUR signals were chosen due to their increasing distance from the epicentre. The change of earthquake characteristics with the distance to the epicentre was investigated. As one moves away from the epicentre, the energy of the earthquake decreases. Notably in this earthquake, the attenuation of the peak accelerations in the EW direction was lower than in the NS direction strongly supporting the unzipping of the fault along the EW direction.

1.Introduction

Kocaeli and the Marmara region were shaken by an earthquake with a moment magnitude of 7.4 on the Richter scale on August 17, 1999 at 3.02am local time. Structural damage occurred in Kocaeli, Adapazari, Istanbul, Eskisehir, Zonguldak and Yalova. The earthquake lasted for 45-50 seconds and was felt as far away as Ankara which is about 300 km away from the epicentre in Golcuk, a suburb which is 11 km south-east of Izmit and 90km east of Istanbul.

Following the earthquake the north strand of the east-west extension of the North Anatolian Fault Zone (NAFZ) which is the Adapazari, Kocaeli, Golcuk segment was seen to have ruptured as shown in Figure 1.1. This ruptured fault is 125 km long and follows the south coast of Izmit bay, extending from Arifiye in Adapazari in the east up to Yalova in the west. Lateral displacements of between 1.9 to 3.0m could be seen and at some places the fault was displaced by 2m vertically.

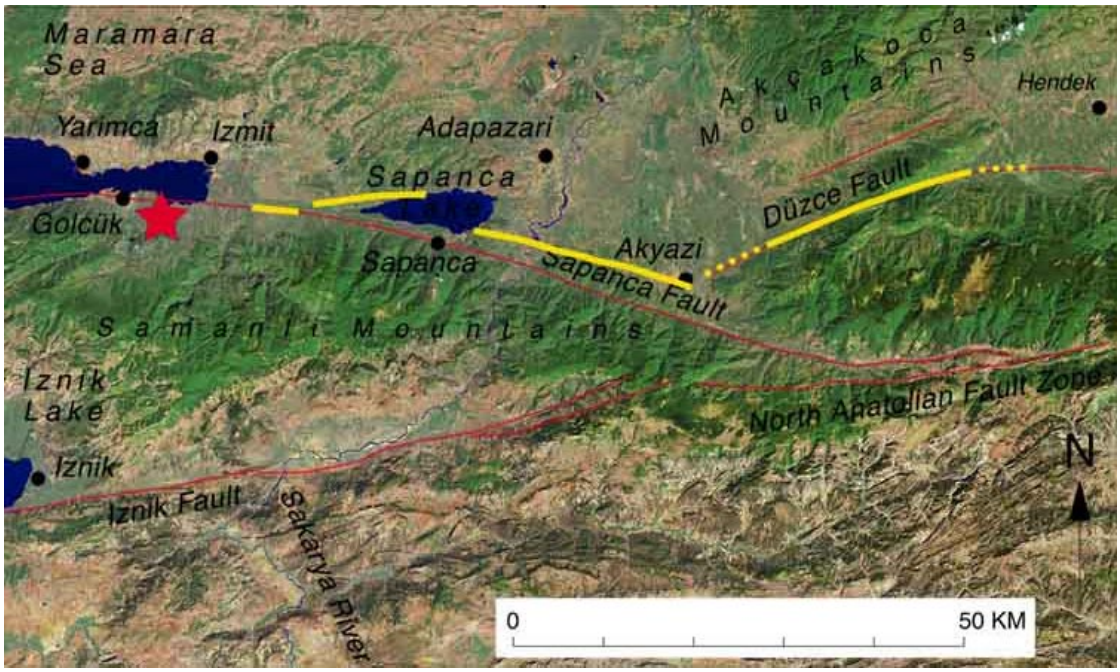

Figure 1.1 Fault rupture map observed by the USGS team. The red lines are previously mapped faults, the red star is the epicentre of the Kocaeli earthquake, and the yellow lines represent the surface ruptures seen. (*http://quake.wr.usgs.gov/study/turkey/rupturemap.html*)

Peak lateral ground accelerations of 0.41g were measured in Adapazari. The main shock was followed by many aftershocks with varying magnitudes. The focal depth of

the main shock was estimated by the USGS as 17km, classifying it as a shallow earthquake. The peak ground accelerations about 10km away from the epicentre at Yarimca Petrochemical Facility were 0.32g in EW, 0.23g in NS and 0.24g in UD.

When analysing the strong motion data acquired from this earthquake, Fourier transform and a time-frequency technique using harmonic wavelets developed by Newland (1999) were applied, and spectral density graphs and wavelet maps were used as visual presentation of the analysed data. In the following sections an introduction to wavelet theory will be presented along with various methods for applying this theory to earthquake acceleration signals for analysis. Finally, conclusions will be drawn with the application of this methodology to the Kocaeli Earthquake, 1999.

2. Methods of Analysis

The majority of signal analysis techniques include signal magnitude, as well as time domain, frequency domain and a combined time-frequency domain analysis. The last two provide detailed information about the signal. Time-domain and frequency-domain constitute two alternative ways of looking at a signal. In the time domain, signals can be analysed in the form of the time histories and identifying signal peaks or any significant property of the signal. In the frequency domain analysis of continuous signals, the time history of a digital signal has to be converted into frequency domain using a Discrete Fast Fourier Transform (DFFT). Fourier transform allows us to switch from one domain to the other; however it does not combine the two domains. (Hlawatsch and Boudreaux-Bartesl, 1992). In the frequency domain, time information is not accessible and it does not provide time localisation of spectral components; it only shows the overall frequency distribution. Using the frequency-time domain it is possible to spot small details of a signal which would not be recognised by any other method. For example, if a time signal had the same frequency of vibrations at two distinct times, such information will show up as a single peak in the DFFT plots. However, in the 3D time-frequency plots using the wavelet method, the frequency peaks would show up as two peaks at two different times. In other words, the localisation of earthquake energy at different frequencies and time instants can be fully represented in one 3-D map.

2.1 Power Spectrum Analysis

Many physical processes or functions, such as ground vibrations, can be described either in the time domain or in the frequency domain. These functions can be defined by the value of h(t) when defined in the time domain or by the amplitude H(ω) in the frequency domain with $-\infty<\omega<\infty$. Their corresponding Fourier transform equations are:

$$H(\omega)= \frac{1}{2\pi}\int_{-\infty}^{\infty} h(t)e^{-i\omega t}dt \tag{2.1}$$

$$h(t)= \int_{-\infty}^{\infty} H(\omega)e^{i\omega t}dt \tag{2.2}$$

where ω is in radians.

Thus, the frequency content of periodic and non-periodic functions can be determined by these Fourier analyses. In the case of non-periodic functions, the function is assumed to be repeatable on either side of the limits of the integral presented in equation 2.1.

2.2 Wavelet Analysis

Wavelet analysis has been found to provide a good method of time-frequency analysis. This is done through a system of combining temporal and spectral domains. In wavelet analysis the signal is broken into a series of local basis functions called wavelets. Wavelets occupy different times and have different frequency compositions so that combined together they completely represent the signal being analysed.

2.2.1 Harmonic Wavelets

Harmonic wavelets have their Fourier transform defined by

$$W_{m,n}(\omega)= 1/(n-m)(2\pi) \quad \text{for } m(2\pi)\leq \omega <n(2\pi)$$

$$0 \quad \text{elsewhere} \tag{2.3}$$

where m and n are real and positive numbers. Inside the band m(2π) to n(2π) the function has constant magnitude which is normalised to ensure the enclosed area to be

unity and outside this band it is zero. The corresponding wavelet function can be defined as follows;

$$w_{m,n}(x)= \{\exp(in2\pi x)-\exp(im2\pi x)\}/\, i2\pi(n-m)x \qquad (2.4)$$

Level m, n indicate a wavelet in the frequency band m(2π) to n(2π) where n>m. In order to form a complete set of wavelets, adjacent wavelet levels must have Fourier transforms with frequency bands touching each other, so that all values of ω along the axis 0 to ∞ are included. (Newland, 1995). Figure 2.2.1 and 2.2.2 show the real and imaginary parts of w(x) defined by equation (2.4) for the case when m=1 and n=2. In the application of these fundamental wavelets for the maps drawn in this paper, a 1-cosine window has been added to the wavelet to give greater localization and to reduce fluctuations extending far from the centre of the wavelet.

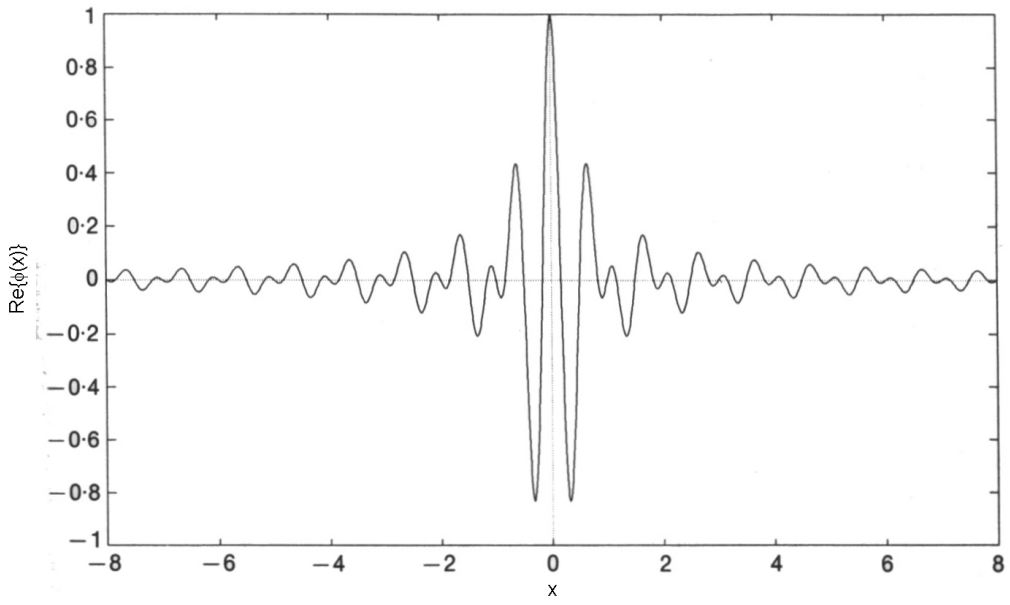

Figure 2.2.1. Real part of w(x).

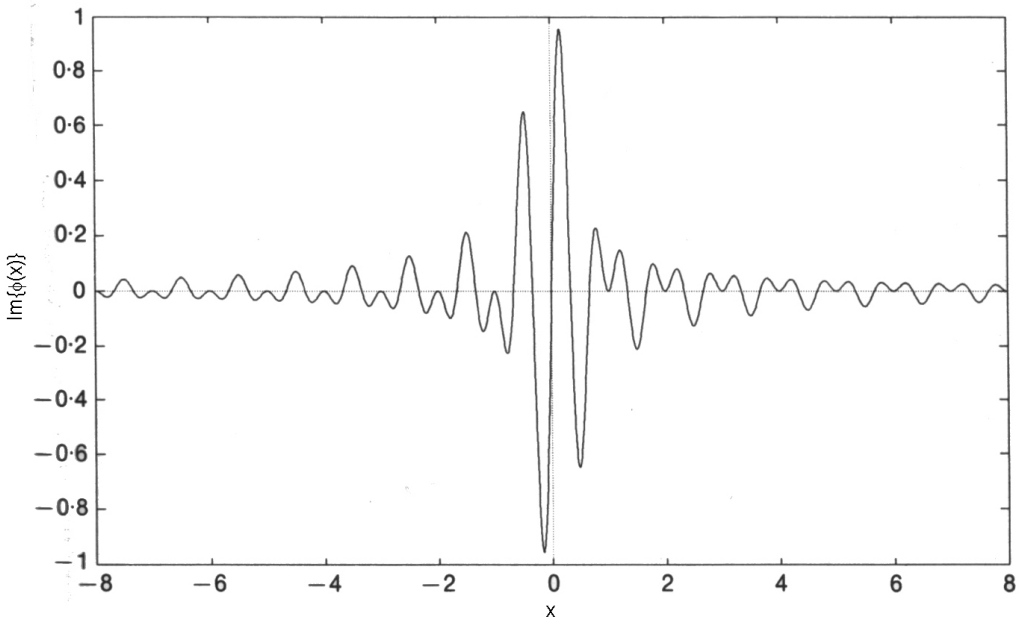

Figure 2.2.2. Imaginary part of w(x).

The FFT algorithm for the calculation of the harmonic wavelet analysis can be seen in the Figure 2.2.3 for an input signal f(t) which is sampled N=16 times.

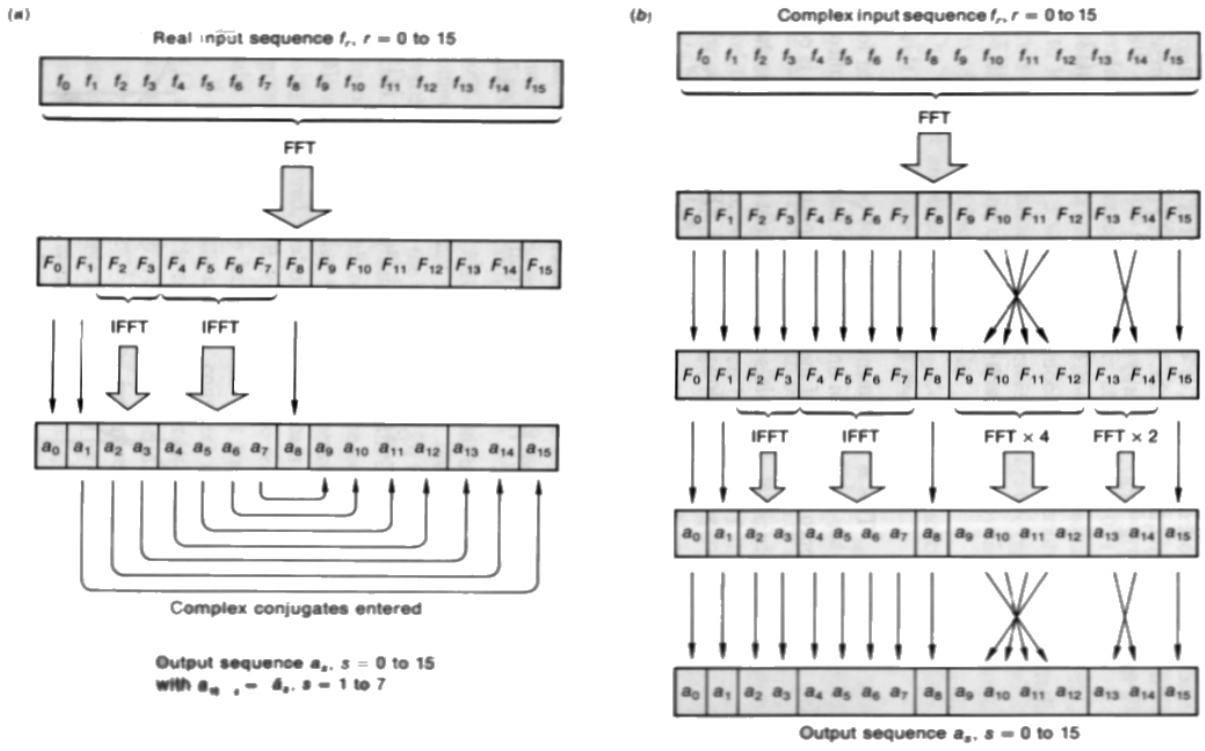

Figure 2.2.3. FFT algorithm to compute the harmonic wavelet transform for a sequence of 16 real and complex elements. (after Newland, 1993)

2.3 Summary

In Fourier analysis, frequency information can only be extracted for the complete duration of a signal f(t). The integral in the Fourier transform equation extends from $-\infty$ to $+\infty$ causing the information it provides in the frequency domain to arise from an average over the whole length of the signal.

If there is a local oscillation in f(t), it will contribute to the Fourier transform $F(\omega)$, but its location on the time axis will be lost. The cause of the value of $F(\omega)$ at a particular ω is not known and it cannot be determined whether it is driven from frequencies present throughout the life of f(t) or during just one or a few selected periods. However in wavelet analysis, this disadvantage is overcome. Through using wavelets, variations in frequency components with time can be observed.

3.The Turkey Earthquake (1999)

The Kocaeli earthquake which occurred on August 17, 1999 has produced many acceleration time histories recorded at various strong motion stations. The main shock was registered by a total of 38 strong motion stations, ten of them were operated by the Kandilli Earthquake Research Centre of Bosphorus University, four of them by the Istanbul Technical University and the rest by the National Earthquake Research Department. The ten records of the Bosphoros University are digitally available from their website which is *http://www.boun.edu.tr*.

Between 6-12 September 1999 a group of academics and professionals who were members of Earthquake Engineering Field Investigation Team (EEFIT), under the auspices of Institution of Structural Engineers, UK, have visited the earthquake affected area to see the effects of the earthquake on engineered and traditional structures. The aim was to quantify the effects, identify the reasons for poor performance of structures and suggest improvements where possible.

3.1 Geology of the Region

A simplified geological map of the key features of the Marmara Region can be seen in Figure 3.1.1. The Adapazari city is located on an alluvial plain which overlies Quaternary Age alluvial deposits with alternating layers of gravel, sand, silt and clay.

The groundwater level is shallow and between 0.5m to 3.0m below ground level. Izmit is located on the northern and eastern side of Izmit Bay, on a coastal plain with a gentle slope to the south, towards the sea. It is underlain by Quaternary age deposits with alternating layers of clay, silt, sand, gravel and a dense silty fine sand. Avcilar, which is about 20km west of Istanbul's city centre, is located on a moderately steeply inclined hillside facing south and east. The geological map shown in Figure 3.1.1 indicates that Pliocene age deposits underlie the Avcilar area and that Quaternary age deposits occur near Bakirkoy and Buyuk Cekmece with unconsolidated sand and gravel. (Kocaeli Earhquake, EEFIT, 2000) Overall, these soil conditions are considered to be problematic for building in such a high seismically active region.

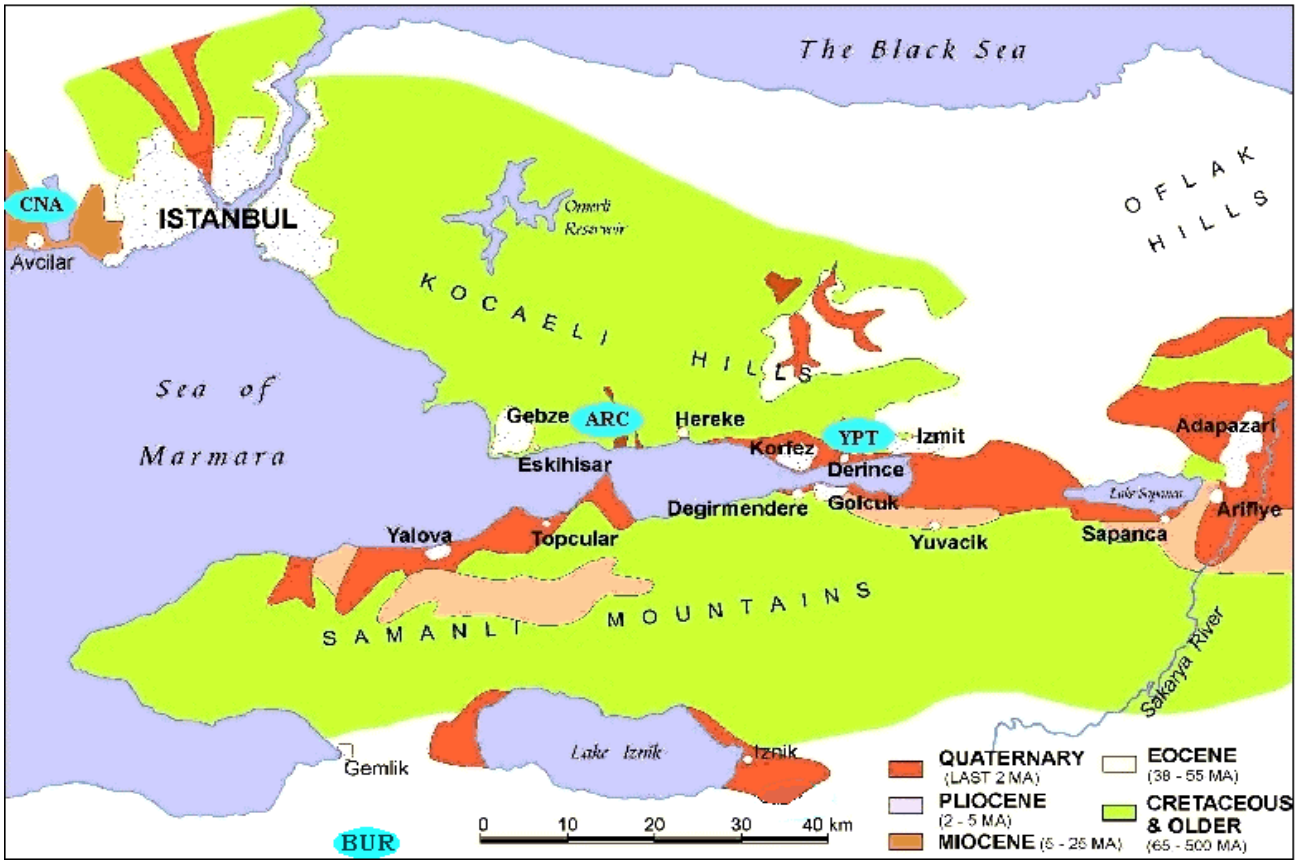

Figure 3.1.1 Simplified geological map of earthquake affected area. (After Kocaeli Earthquake, EEFIT, 2000)

3.2 Strong Motion Data

The Izmit Meteorology Observatory has recorded maximum accelerations of 0.163g in NS, 0.22g in EW, and 0.123g in UD directions. Gebze station has recorded 0.261g in NS, 0.14g in EW, 0.179g in UD and Adapazari station 0.407g in EW (which was the maximum acceleration observed in this earthquake), and 0.259g in UD directions. Unfortunately, strong motion recording instruments were sparse in the area where the damage was particularly severe. No data was available for Golcuk and its vicinity, the epicentral area.

The location of the strong motion stations are as shown in Figure 3.2.1. The station nearest to the epicentre was located at the Yarimca Petrochemical facility (YPT) and was visited during the EEFIT mission, along with the Arcelik and Gebze stations. The instrument was placed on the ground floor of a three story high building in YPT. Gebze station, which is 35km away from the epicentre, measured 0.261g as peak acceleration in north-south direction, and the seismograph was placed on the ground floor of a one-story building. In Arcelik (ARC) the instrument was placed under a single story building which was isolated from its foundation by springs and measured 0.211g in NS. These signals used do not represent free-field conditions since they are all based within a building usually on the ground floor of a one or two-story building. The peak accelerations registered can also be seen in Figure 3.2.1. The records obtained from some of the strong motion stations can be seen in Figure 3.2.2 and in detail for YPT, ARC, Bursa Tofas Factory (BUR) and Cekmece Nuclear Centre (CNA) in Figures 3.2.3 a, b, c and d. These acceleration-time histories are only for the first 80 seconds of the earthquake. The sampling rate of the signals was 200Hz.

In this report YPT, ARC, CNA, and BUR signals were closely investigated. The reason these four stations were chosen among ten signals is due to their distance from the epicentre with YPT station being the nearest to the epicentre and BUR station the farthest. Therefore the change in the earthquake accelerations at YPT and BUR stations and the behaviour of earthquake as it progressed away from the epicentre could be investigated. BUR station is located in the south-west and CNA in the north-west of the epicentre. The locations of these stations is shown in Figure 3.1.1.

As can be seen from the records, YPT and ARC, which were located very close to each other (about 25km apart), and have recorded the peak acceleration in EW

direction as 0.322g and in NS as 0.211g respectively. The attenuation of the signals is significant due to discontinuity in the geological formations and sedimentary deposits near the stations as seen in Figure 3.1.1. The YPT station was nearer to the coast of Marmara where as the ARC station was towards inland.

YPT shows two distinctive peaks which might mean two particular earthquakes as seen in Figure 3.2.3a. The first peak was at 10 seconds, then the second one at 42 seconds yielding the time between the two events of about 30 seconds. A similar trend is also seen in ARC traces in Figure 3.2.3b. At the CNA station the maximum acceleration was registered in NS as 0.177g and had two peaks at 21 and 49 seconds as shown in Figure 3.2.3c. The trace from BUR station seen in Figure 3.2.3d has recorded in NS 0.101g as the maximum acceleration, but did not show the two peaks clearly; only at 23 and 50 seconds could the peaks be spotted.

Comparing the ratios of the peak accelerations acquired in each direction between YPT signal and the others, the maximum ratio acquired between the NS components of YPT and ARC signals is 0.92. Table 3.2.1 shows the attenuation factors with respect to YPT station which is the closest to the epicentre being only 10 km away.

Table 3.2.1 Normalised accelerations with respect to acceleration at YPT station.

Station	N-S	E-W	U-D	Epicentral Distance
ARC	0.92	0.41	0.35	35
CNA	0.77	0.41	0.24	105
BUR	0.44	0.31	0.2	130

Attenuation in NS direction is as expected, further we go, there is attenuation in peak accelerations due to damping (material and geometric damping). However in the EW direction the rate of attenuation is much smaller in this direction. This is an interesting feature which will be investigated thoroughly later on. The reason why the ratios are smaller in EW direction can be explained by the unzipping of the fault along the EW direction, pumping more energy in that direction. Hence it appears as if there is less attenuation in that direction. The UD ratios also attenuates away from the epicentre.

Looking at the components of the signal at YPT station prior to the first peak (10 seconds into the record, Figure 3.2.3a), the UD component is shown to contain more oscillations than the NS or EW components. The instrument could have picked up the P-waves which travel faster than S-waves and consequently arrive earlier. UD component is induced by different kinds of stress waves namely, P. This is also

observed in UD component of ARC signal in Figure 3.2.3b, but this time NS component has picked up oscillations. This is interesting because the fault line runs in an EW direction.

In CNA and BUR signals shown in Figure 3.2.3c and 3.2.3d respectively UD components picked up oscillations before the peak accelerations like YPT and ARC signals, again due to the velocity of wave types. Repetition of this point in all the signals suggest P-waves due to the ground motion has reached the stations before the horizontal waves.

When you compare the ARC and YPT signals in Figures 3.23a and 3.2.3b respectively even though they both show the two peaks ARC signal has peak accelerations after 10 seconds at 14 seconds. This difference represents the time passed for the main shock to reach ARC. The peak acceleration reached CNA station at 21 seconds and BUR station at 23 seconds.

The presence of peak accelerations in UD before the peak accelerations reached by NS and EW components show that the vertical accelerations occur before the horizontal accelerations. The vertical accelerations are a result of the primary waves (P waves) within the soil layer arised by the earthquake motion. The horizontal accelerations result from the shear waves (S waves) within the soil layer.

Acceleration records acquired from the Kocaeli Earthquake can be seen in Table 3.2.2.

Table 3.2.2. Acceleration Records from Kocaeli Earthquake.

Location	Distance from The Fault (km)	Peak Acceleration (g)
Adapazari	40	0.410
ARC(Gebze)	35	0.211
Atakoy	105	0.168
ATS(Ambarli)	105	0.252
BTS(M.Ereglisi)	185	0.099
BUR(Bursa)	130	0.101
CNA(Cekmece)	105	0.177
DHM(Yesilkoy)	105	0.090
Duzce	105	0.373
FAT(Fatih)	90	0.189
Gebze	35	0.261
Goynuk	79	0.137
HAS(Heybeliada)	70	0.143
Izmit	5	0.219
Iznik	35	0.126
YKP(Istanbul)	90	0.041
YPT(Yarimca)	10	0.322

All the acceleration traces have shown two significant peaks suggesting two earthquakes which happened with 30 seconds between each event. Geotechnical condition under the strong motion data stations may have affected the observed ground oscillations. The distance to the epicentre effects the arrival time of the main shock to each point observed. The signals give a chance to investigate the travel of stress waves away from the epicentral zone. The vibrations before the peak acceleration is observed at the UD signals of each record analysed suggest the arrival of P waves before the S waves in all places.

Figure 3.2.1 Strong ground motion stations and the peak horizontal ground acceleration (%g) registered by them during the Kocaeli Earthquake, 1999.

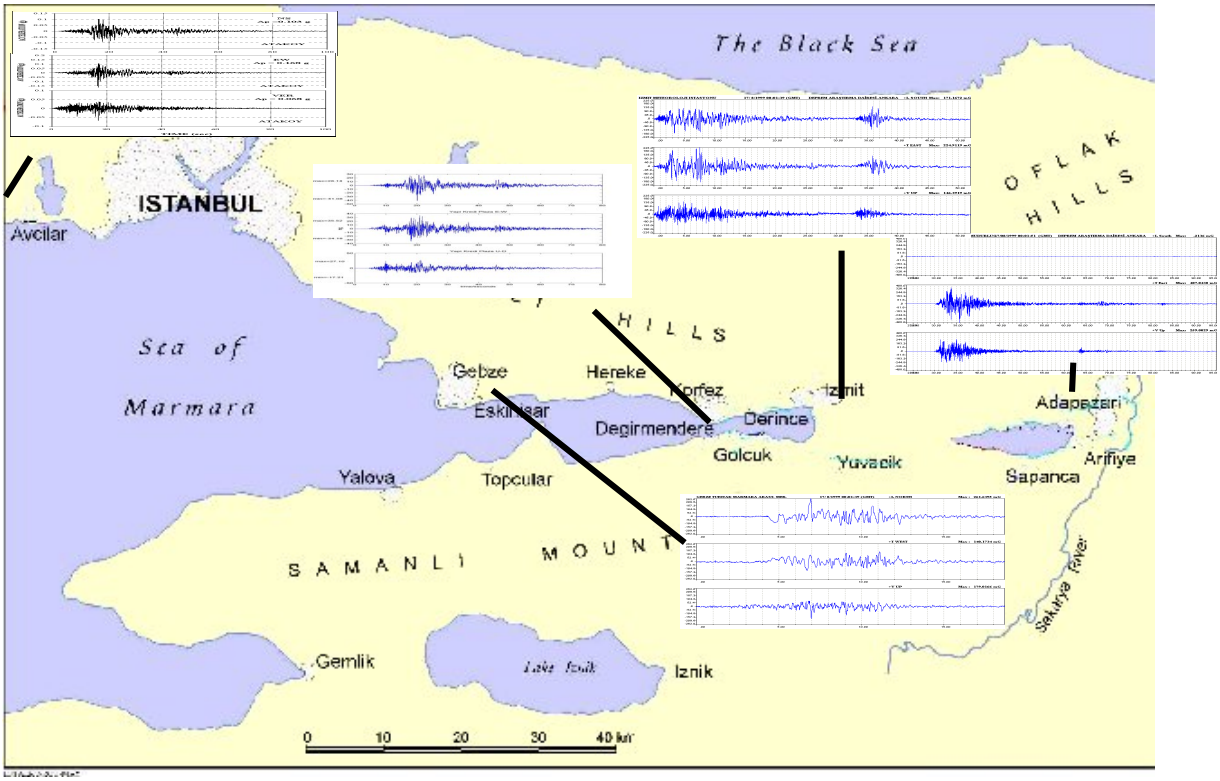

Figure 3.2.2 Map of the region with some acceleration traces.

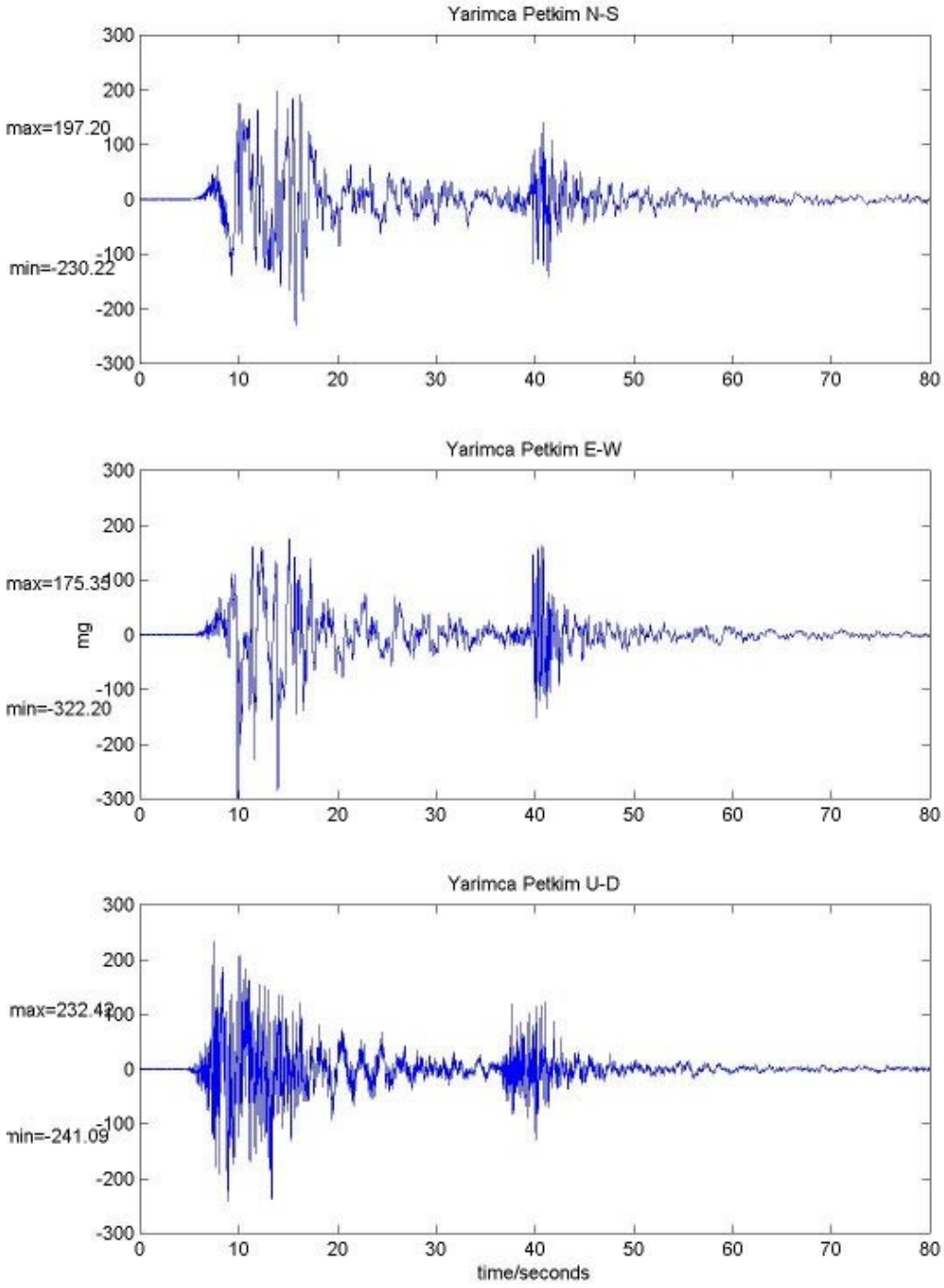

Figure 3.2.3a. The acceleration time history of YPT station.

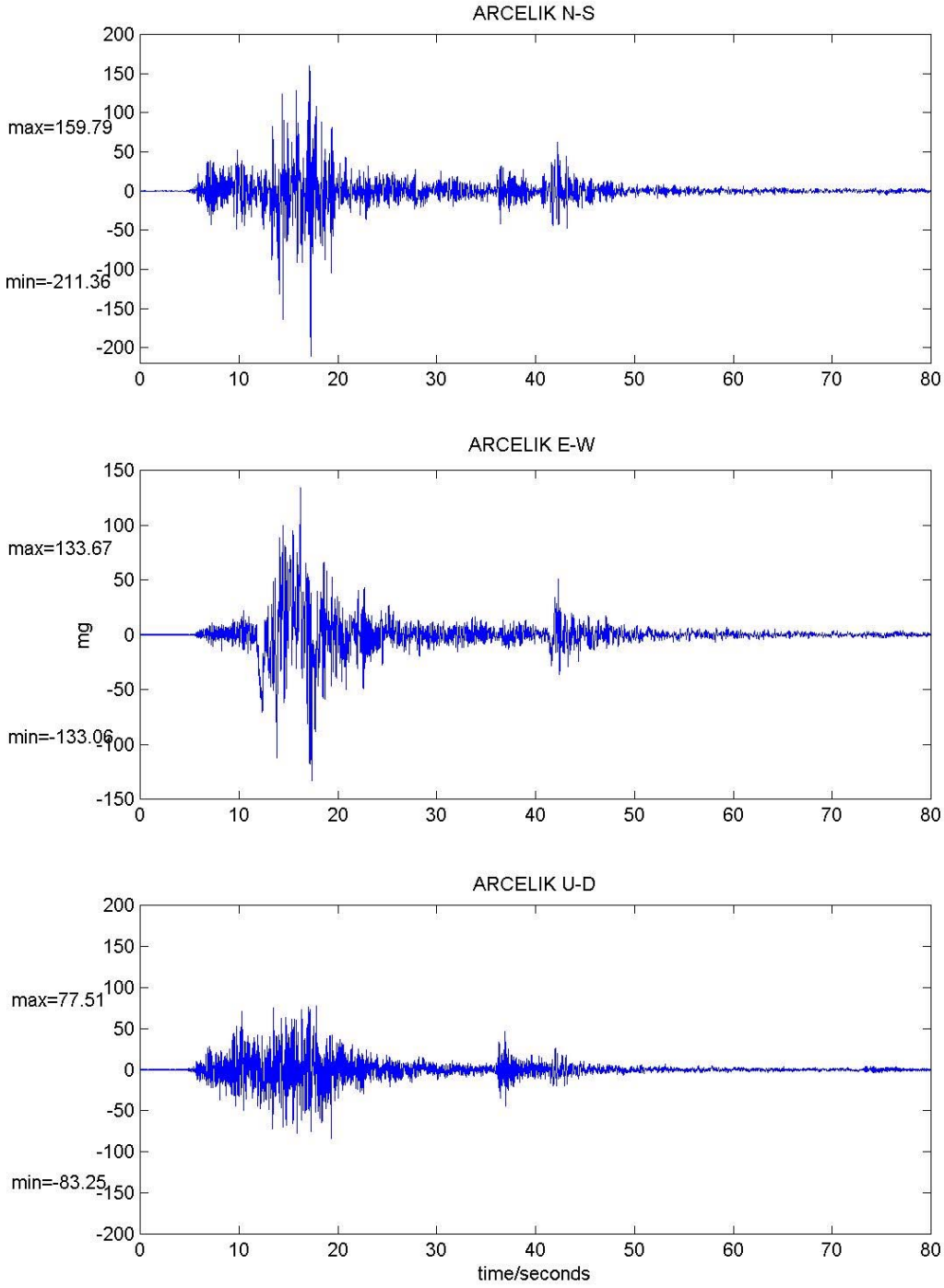

Figure 3.2.3b The acceleration time history of ARC station.

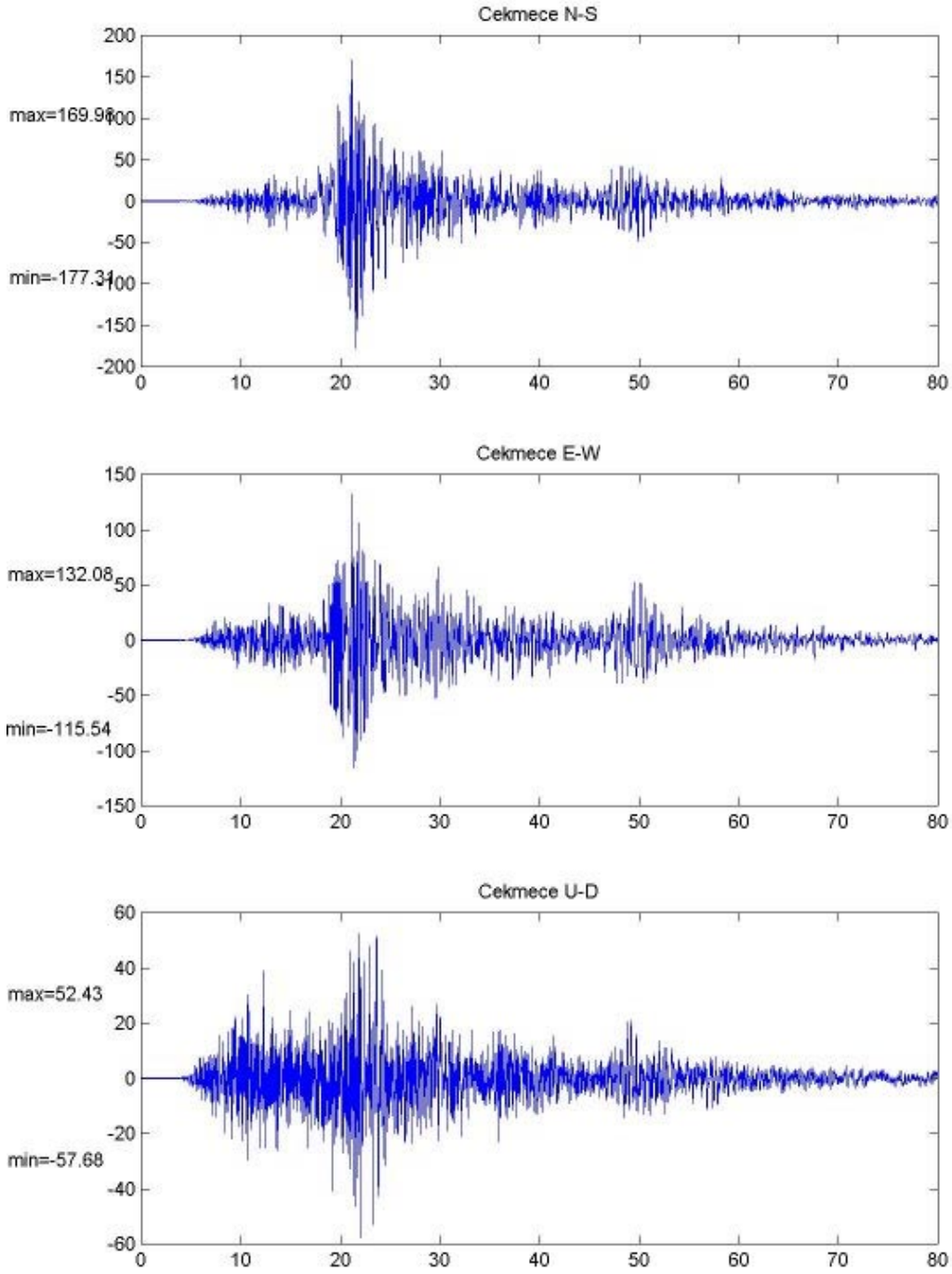

Figure 3.2.3c The acceleration time history of CNA station.

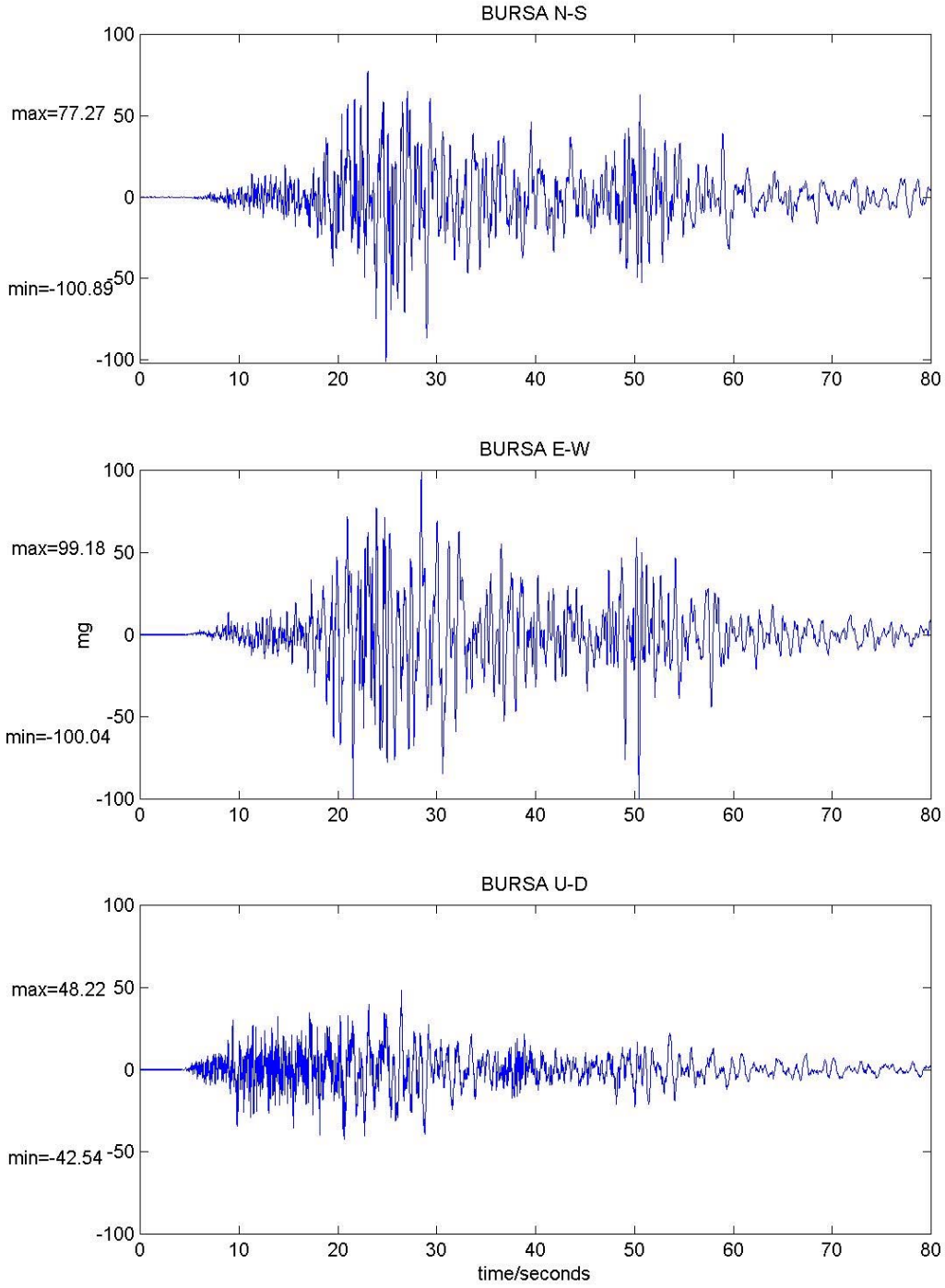

Figure 3.2.3d The acceleration time history of BUR station.

3.3 Fourier Analysis

Frequency analysis using FFT method was carried out on N-S, E-W and the U-D components showing various frequencies between 0-10 Hz. Figure 3.3.1-3.3.4 show the results of the frequency analysis of the signals from YPT, ARC, CNA and BUR stations. The frequency contents of the YPT signals seen in Figure 3.3.1 show the first peak at 0.3Hz, 0.125Hz and 0.4Hz for NS, EW and UD components respectively. With ARC signals seen in Figure 3.3.2 it was difficult to pinpoint one significant frequency, various frequencies being observed. The dominant frequencies were, in NS 0.1 and 0.7Hz, EW 0.6 and 0.7 Hz and in UD 0.5Hz. For the CNA signals seen in Figure 3.3.3 the NS component had a peak frequency at 5Hz, while with the other components the peaks cannot be easily identified. The BUR signals in Figure 3.3.4 had different peak frequencies, namely 0.1 Hz, 0.7 Hz and 1.5 Hz for NS, 0.6Hz and 0.8 Hz for EW and 0.4 and 0.5Hz for UD. These graphs show that there are various frequencies present for the duration of the earthquake. There is no one dominant single frequency in the signals. As one moves away from the epicentre, the frequencies change.

UD component of YPT signal contains significant high frequencies between 4.5-5.5Hz. ARC signal has similar frequency graphs with significant frequencies present between 3-7Hz for NS, EW and 0-1Hz for UD. When YPT and ARC are compared, the frequency content of YPT signal is concentrated below 1Hz, decreasing in magnitude at higher frequencies, whereas ARC signal has peak energies at two higher frequencies. CNA signal has significant frequency contents between 1-8Hz. For NS, the peak is at 5Hz. For EW at 1.5Hz and 3.5Hz. BUR signal has the same trend as YPT between 0-3Hz. Higher frequency component die down quickly.

Magnitude of acceleration at different frequencies decreases as one moves away from the epicentre, meanwhile higher frequency contents increases. This maybe due to the local geology and super-structure where the strong motion data instruments are placed. As a result site specifications can influence the measurements you get as well as the epicentral distance. All the UD components have higher frequency contents than the other horizontal components since they are composed of P-waves which travel faster.

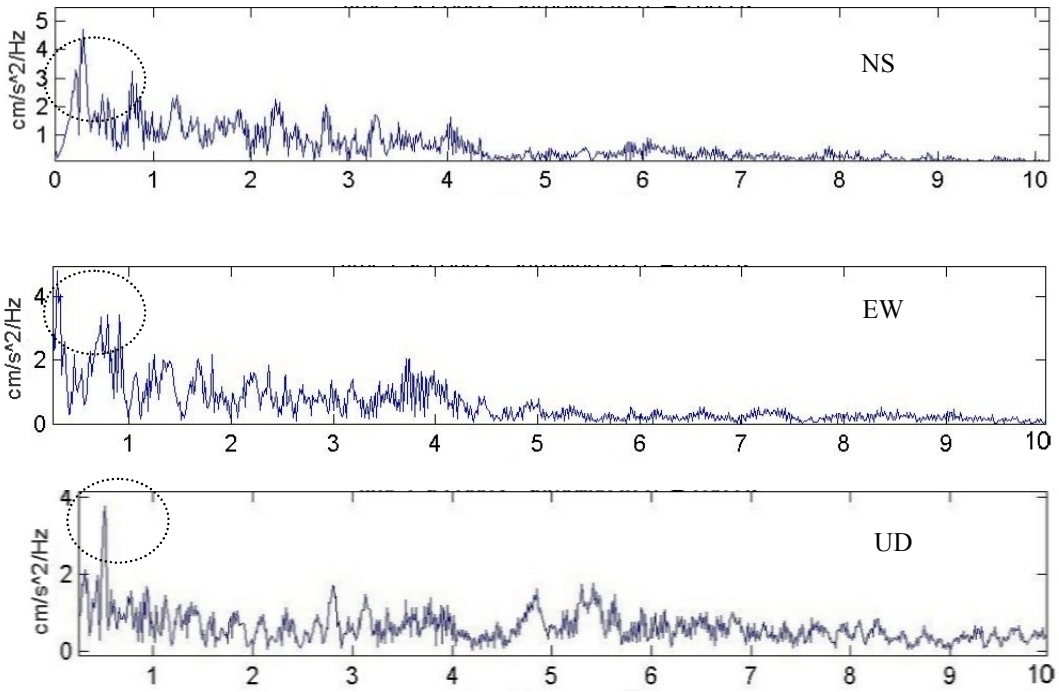

Figure 3.3.1 Fourier analysis of YPT signal. 10 km from the epicentre.

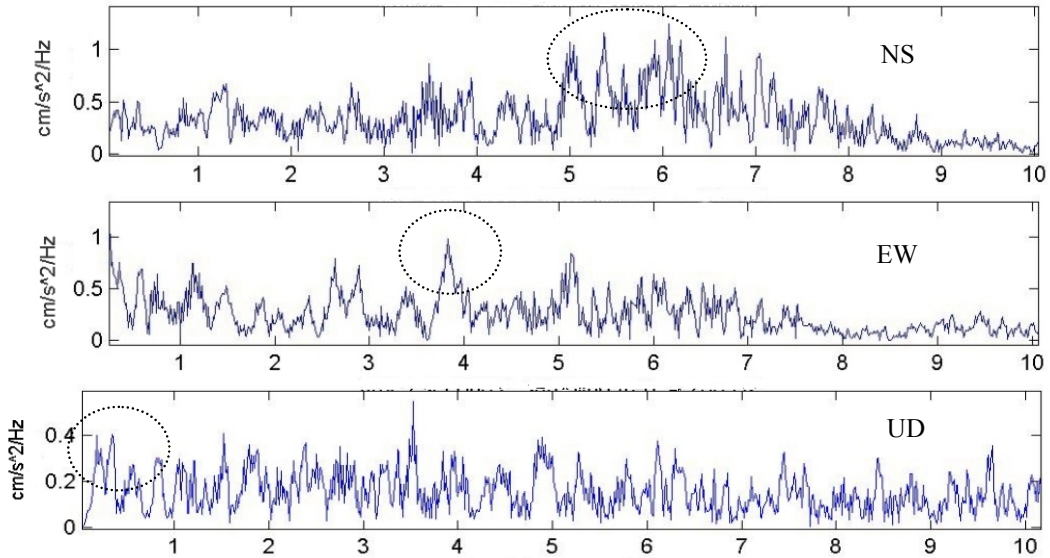

Figure 3.3.2 Fourier analysis of ARC signal. 35 km from the epicentre.

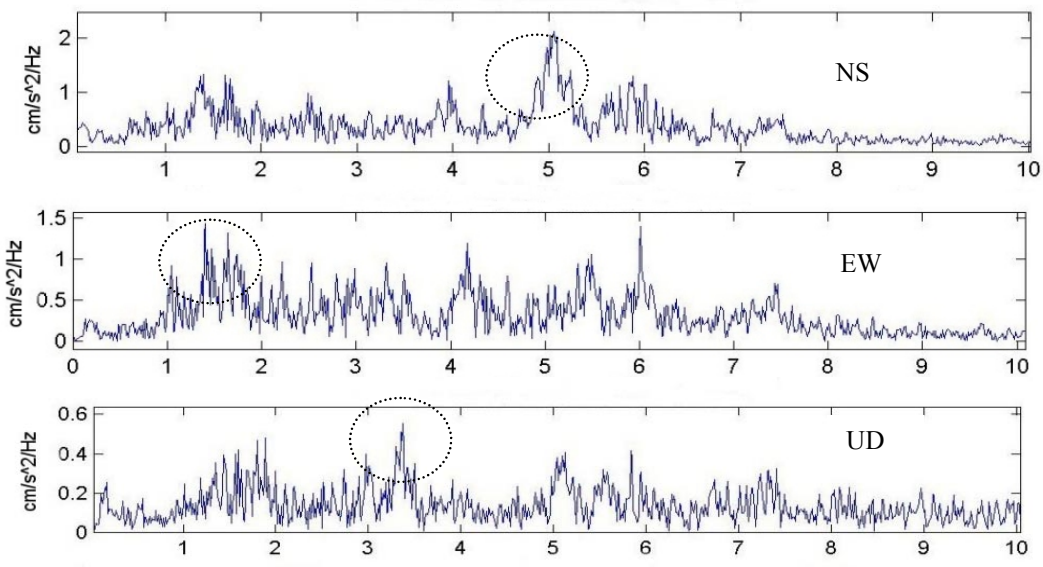

Figure 3.3.3 Fourier analysis of CNA signal. 105 km from the epicentre.

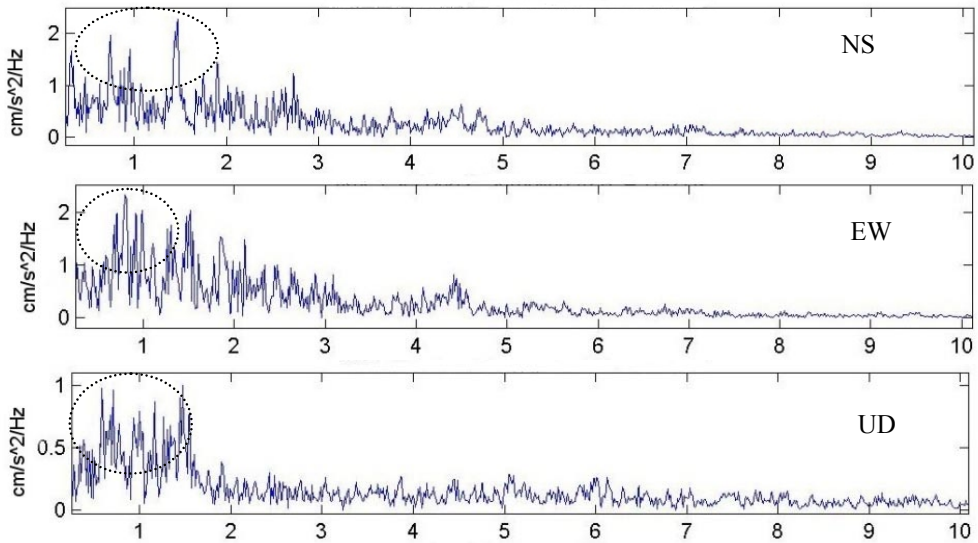

Figure 3.3.4 Fourier analysis of BUR signal. 130 km from the epicentre

3.4 Wavelets

The wavelet program used, computes the harmonic wavelet transform of the record and plots the result as the time-frequency map covering the whole frequency range from 0 to Nyquist frequency. It differs from the basic harmonic wavelet described above by windowing, so that the slope of the wavelet is as shown in Figure 3.4.1. This detail is described in Newland (1998 and 1999b). In their simplest form, orthogonal harmonic wavelets provide a complete set of complex exponential functions whose spectrum is confined to adjacent (non-overlapping) bands of frequency. In their practical application, the boxcar spectrum of harmonic wavelets is smoothed (to improve localisation in the time domain) and the spectra of adjacent wavelet levels are overlapped to give over-sampling in order to improve time-frequency map definition. These wavelets have been found to be particularly suitable for vibration and acoustic analysis because their harmonic structure is similar to naturally-occurring signal structures and therefore they correlate well with experimental signals. They can also be computed by a numerically-efficient fft-based algorithm. A typical wavelet is shown in Figure 3.4.1. Its centre frequency, bandwidth, and frequency weighting can be adjusted as required to match the underlying characteristics of the signals being analysed.

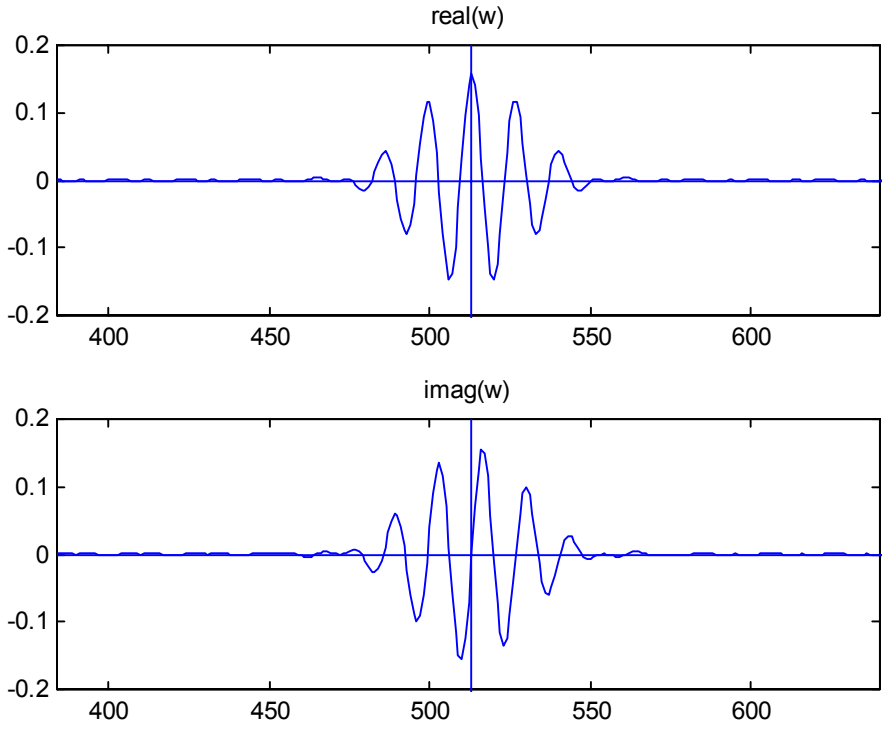

Figure 3.4.1 Specimen harmonic wavelet: Real part above, imaginary part below.

Time-frequency maps plotted in this report are the two-dimensional contour diagrams of the three-dimensional surface plots created from the harmonic wavelet transform calculations. The axes of the map are time plotted horizontally and frequency plotted vertically. Different colour shadings represent the various contour levels.

Figure 3.4.2-3.4.5 show the results of harmonic wavelet analysis for the signals from YPT, ARC, CNA and BUR stations. It must be pointed out that the colour scale is different for different plots, to maximise the resolution for each plot. In Figure 3.4.2 the first acceleration of YPT signal has a peak frequency of 0.3 Hz, and the second event a peak frequency content of 1Hz for NS observed at 10 and 42 seconds respectively can be seen. In the EW direction the first peak had a peak frequency of 0.125Hz and 1Hz at 10 and 42 seconds. These two events have different frequency contents at different times which can not be detected with Fourier analysis. Same frequency present at different times, and secondly, the presence of various frequencies at the same time can also be observed which cannot be distinguished by FFT. With ARC signals, too many frequencies are present in the same time period especially for the 10-20 seconds period. All components show the same trend. Components of the CNA signal show many frequencies between 10-30 seconds of the earthquake. However the NS component has two peaks at 1.2Hz and 5Hz and the time zones with frequency bands are not constant. For the BUR signal, the frequency band of 0-2Hz is quite effective over 20-35 seconds for all the components.

When one looks at the NS, EW, and UD components of YPT signal, two significant time bands involving various frequencies can be seen. The first one is between 8-20 seconds and then between 38-48 seconds. The 0-5 Hz frequency band is significant over 8 to 60 seconds of the NS and EW signal where this band extends to 8Hz for 5-50 seconds. These were not visible with the FFT graphs.

In NS and EW components of ARC signal has a signal time band between 8-22 seconds. 0-10 Hz frequency band is significant over 8-60 seconds. In UD signal it is a triangular pattern between 0-30 Hz and 5-80 seconds. If UD signal is mainly composed of P-waves, since they arrive quickly, they die down quickly, too. This might be an explanation of this observed pattern.

When you compare YPT and ARC signals, these two signals have different time-frequency patterns which would not be obvious or achieved by acceleration traces or

frequency graphs alone. As a result of the Fourier analysis the frequency content of the second peak was lost. With the frequency-time maps achieved by wavelet analysis this could be seen. The frequency content of peak accelerations can also be observed.

In NS and EW components of CNA signal have 0-10Hz frequency band between 10-80 seconds. Then EW component has various frequencies between 10-20Hz with UD components, various frequencies are present through the whole signals with significant time zones between 10-30 seconds. YPT and CNA signals both have different time-frequency patterns.

When one looks at the NS and EW components of BUR signal, only the 0-6Hz frequency band between 10-60 seconds was significant, with concentrations between 20-30 and 50-60 seconds. UD component has a significant frequency band between 0-2Hz and between 10-60 seconds. It also has the 0-6Hz band between 10-60 seconds like NS and EW components. When YPT compare with BUR, they both have different pattern. UD signals always contain the higher frequencies.

In summary, all the signals have different time-frequency patterns not seen in the FFT analysis. Also the frequency content at each time interval could be observed. All frequencies concentrated between 10-20 seconds of the earthquake for YPT and ARC and between 20-30 seconds for CNA and BUR signals. Energy spreads out as you go away from the epicentre. YPT has short, sharp peaks. Higher frequency damps out quickly and CNA signal shows the energy is spread over time suggesting soil amplification could have occurred in that region.

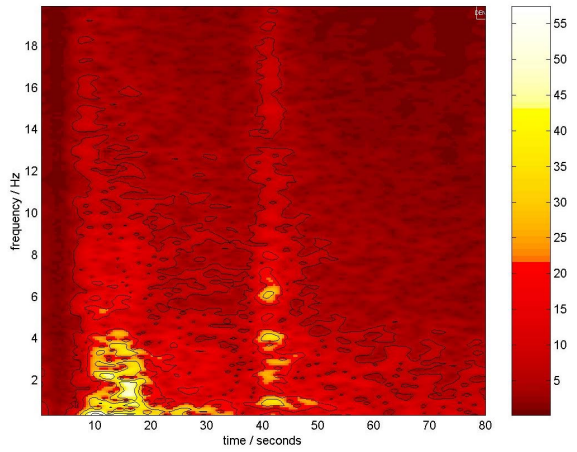

(N-S)

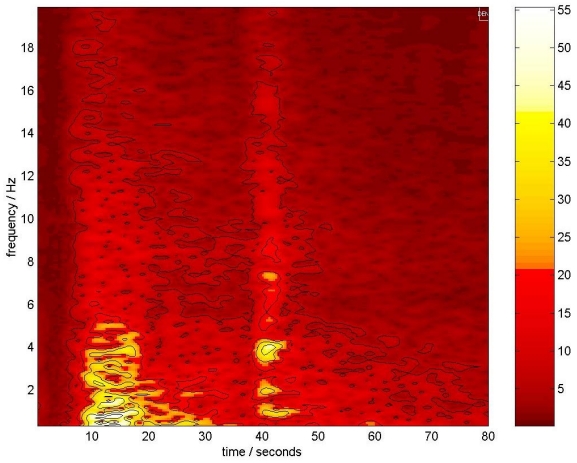

(E-W)

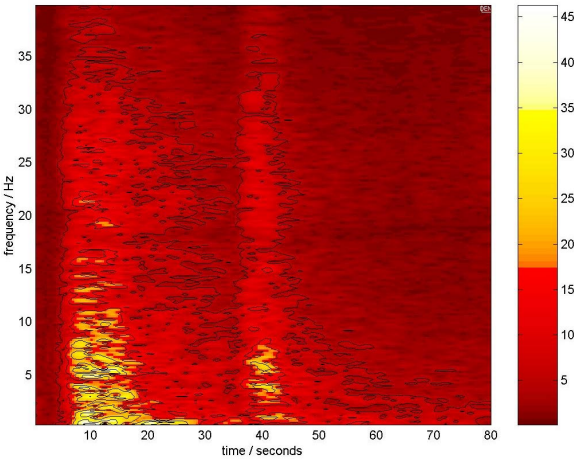

(U-D)

Figure 3.4.2 Wavelet analysis of YPT signal. NS, EW and UD components respectively.

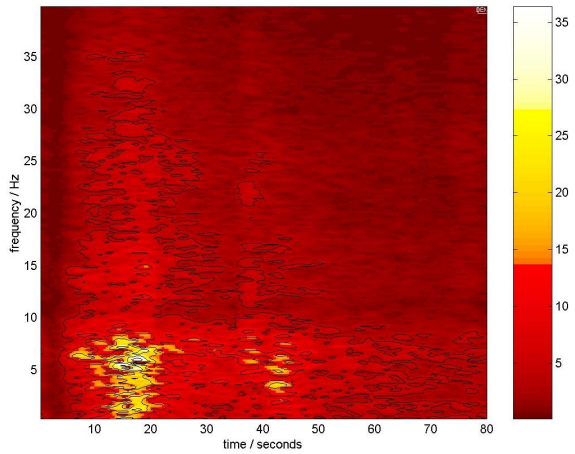

(N-S)

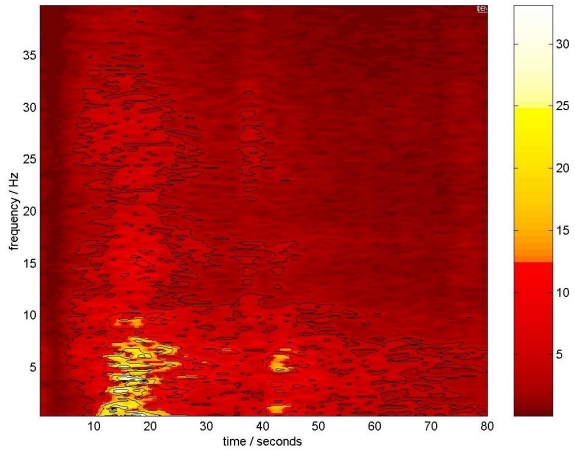

(E-W)

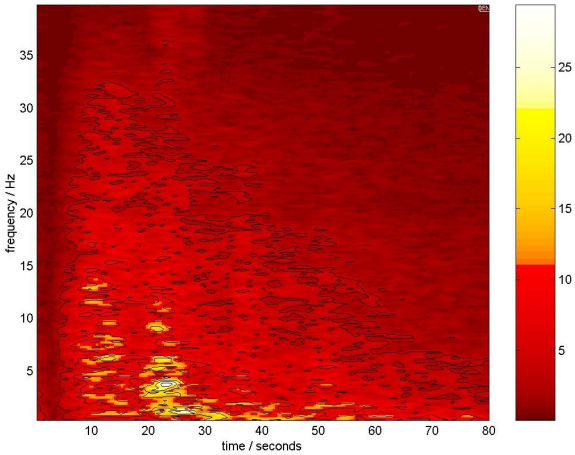

(U-D)

Figure 3.4.3 Wavelet analysis of ARC signal. NS, EW and UD components respectively.

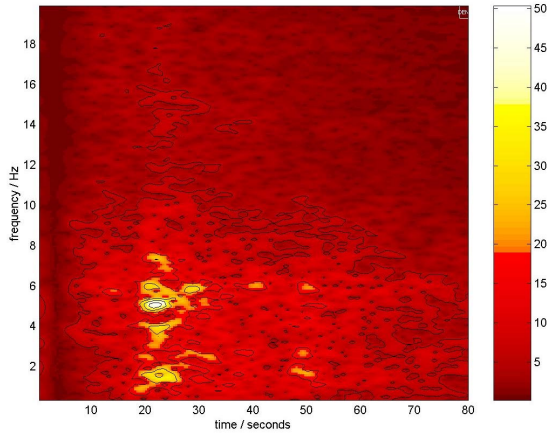

(N-S)

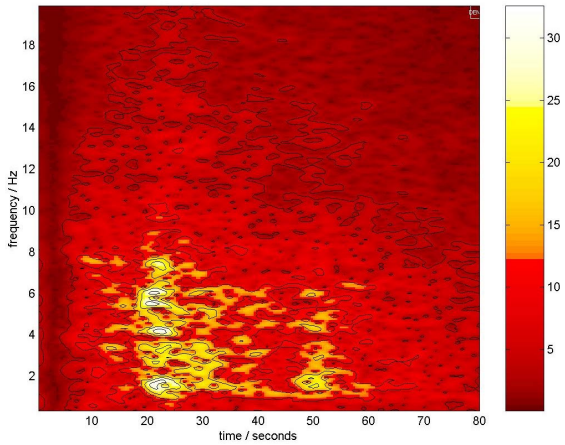

(E-W)

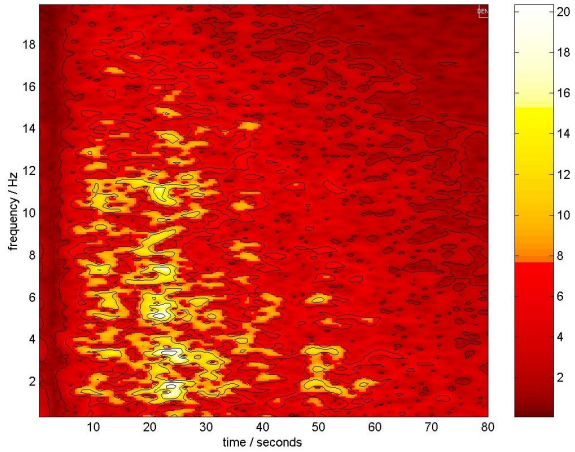

(U-D)

Figure 3.4.4 Wavelet analysis of CNA signal. NS, EW and UD components respectively.

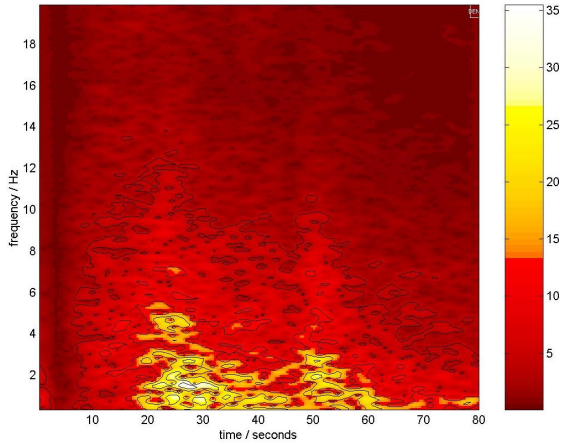

(N-S)

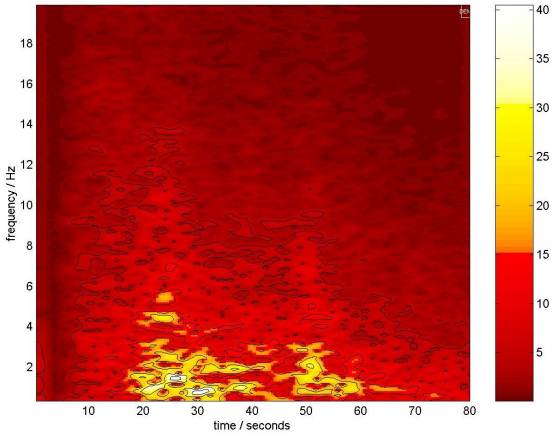

(E-W)

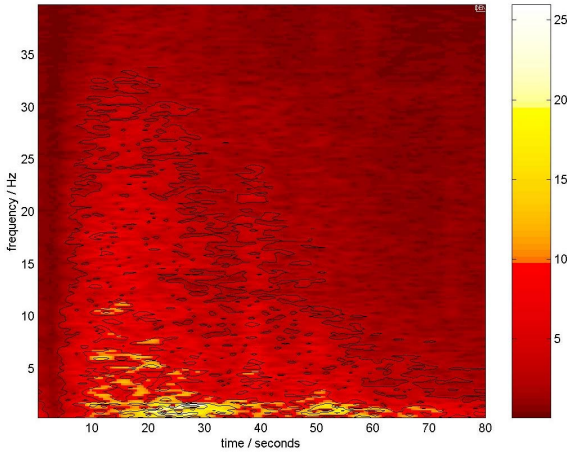

(U-D)

Figure 3.4.5 Wavelet analysis of BUR signal. NS, EW and UD components respectively.

3.5 Particle Acceleration Trajectories

NS component of each signal is plotted against EW component to observe the phase relationship of the signals in different time windows. If the signals are in phase, the figure will be a diagonal line inclined at 45° and if they are not in phase, the line opens into an ellipse as phase difference increases. As the ellipse becomes a circle, the phase difference will be 90° and if the ellipse tilts to the opposite direction the phase difference increases to 135°. To investigate the phase relationship between the NS and EW components of the acquired signals particle acceleration trajectories were constructed by plotting EW component along the x-axis and the NS component along the y-axis as shown in the Figures 3.5.1 and 3.5.2. YPT and ARC signals were chosen since they were the ones nearest to the epicentre and to each other. Figures 3.5.1 and 3.5.2. show the particle acceleration trajectories of the YPT and ARC stations for the Kocaeli earthquake.

For YPT and ARC signals, NS against EW were plotted for the 5-20, 20-35, 35-50 seconds time windows. The change from a NW direction to EW and then to SE direction was observed in YPT signal as shown in Figure 3.5.1. The direction of the earthquake changes from a NW direction to SE movements as seen in Figure 3.5.2.

The particle acceleration trajectories of the records were plotted for a range of 15 seconds. From these plots the rotational nature of the particle acceleration can be observed along with the phase differences occurring with time.

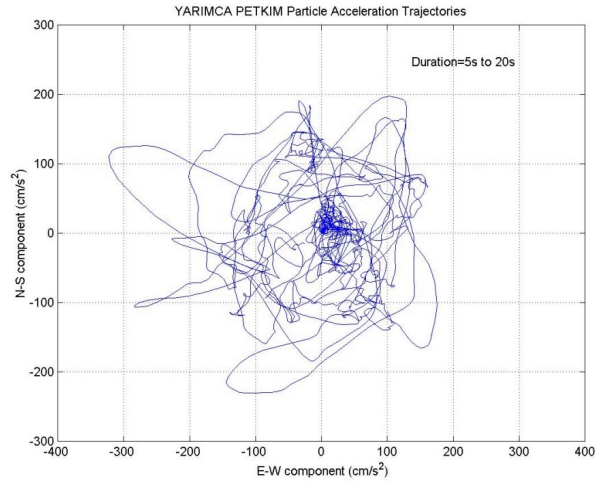

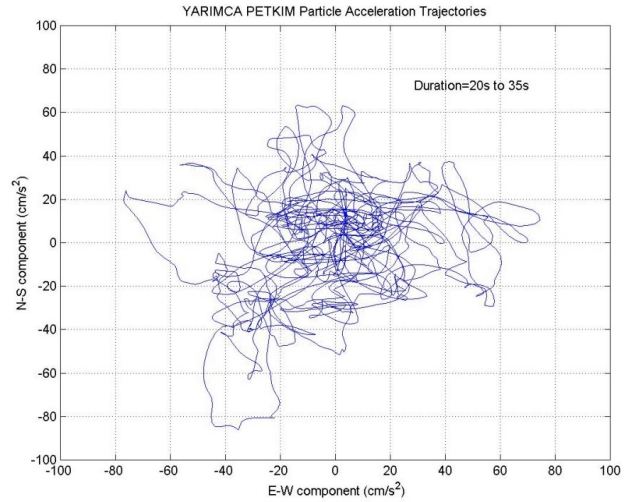

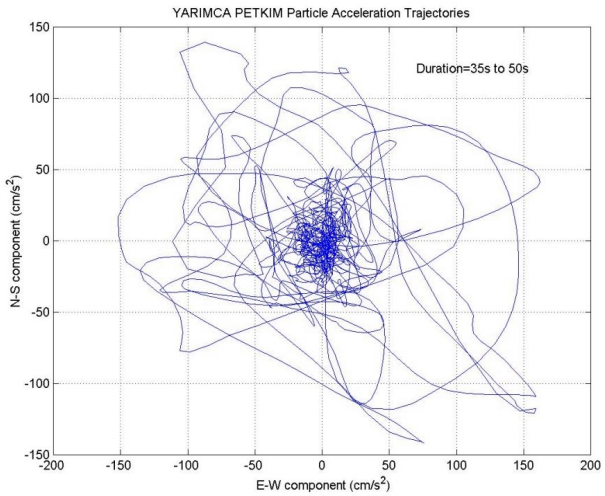

Figure 3.5.1 Particle acceleration trajectories for YPT NS and EW components for the duration of 5-20, 20-35 and 35-50 seconds respectively.

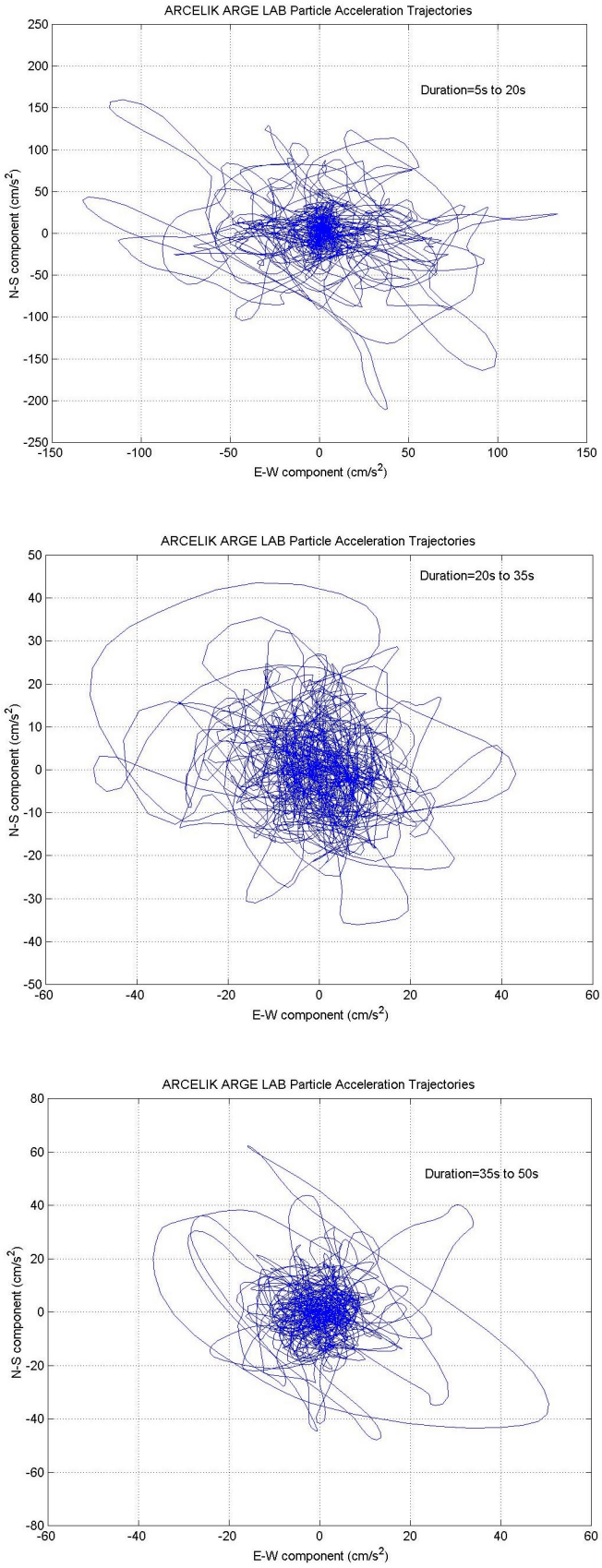

Figure 3.5.2 Particle acceleration trajectories for ARC NS and EW components for the duration of 5-25 and 35-50 seconds respectively.

3.6 Energy caused by the Earthquake

The mesh plots which are 3-D visualisation of time-frequency plane from wavelet analysis is presented in Figure 3.6.2. It must be pointed out that the colour scale is different for different plots to maximise the resolution for each plot. Using both of the figures a comparison of energy distribution can be made. With the summation of the velocity method for the YPT and ARC signals the significant shaking lasts for 15 seconds as seen in Figure3.6.1a and 3.6.1b, while for the CNA and BUR signals the significant shaking lasts about 40 seconds as shown in Figure 3.61c and 3.6.1d.

The energy in the signal, YPT can be seen by the mesh plot, Figure 3.6.2a, where the build-up of energy can be seen between 5-20 seconds, indicating the duration of strong shaking to be approximately 15 seconds. This energy build-up can be seen in Figure 3.6.1, which were constructed by summing the square of the velocity over time. In this graph two energy jumps can be seen, indicating the two consecutive energy releases from the source. 80% of the energy was reached after the first event and the rest from the second event.

Conversely, using the wavelet transform, it can be seen that the two peak points for Arcelik E-W are located at 15 and 45 seconds. It should be noted that these peaks cannot be seen in the Summation of the Velocity Traces technique. This occurs as a result of the fact that for the Summation of the Velocity Traces technique, one is summing over the whole period with the energy of the second peak added onto that of the first peak.

NS, EW and UD components of YPT signal seen in Figure 3.6.2a have two significant mountainous areas representing a continous band of energy at 20 and 50 seconds running along the whole frequency axis. This character was lost in FFT analysis due to the lack of the ability in representing the signal in a time-frequency plane.

The ARC signal seen in Figure 3.6.2b shows one significant mountain at 20 seconds in NS and EW directions. In UD, it is a continuos area over 0 to 40 seconds. CNA signal has one peak at 30 seconds, but this time the mountainous area is between 0 to 8 Hz. EW has significant peaks and the acceleration between 0-8Hz as seen in Figure 3.6.2c. UD mountainous area all over the plane signifying the presence of energy for

the signal. In BUR signal shown in Figure 3.6.2d, NS, EW and UD have peaks along 0-5Hz over the whole duration of the signal.

Height and colour defines the amplitude of the energy in 3D mesh plots. The colour bar shown on the right of the figures signifies the energy in the signals. The energy of a signal can be broken into its contributions from different frequency bands and time locations via wavelet analysis, giving insight into the localised portions of the signal.

The graph seen in the Figure 3.6.3 shows the normalised energies reached by the two methods for the same stations. For the basis acceleration, the data acquired from YPT was chosen as it was the closest available signal to the epicentre. As one distances from the epicentre, the energy decreases as does the intensity of the earthquake.

The energy distribution was observed and the percentage of energy reached after the first event was observed as 80% of the total energy. The energy of a signal was broken into its contributions from different frequency bands and time locations via wavelet analysis and two significant mountainous areas representing a continuos band of energy was observed.

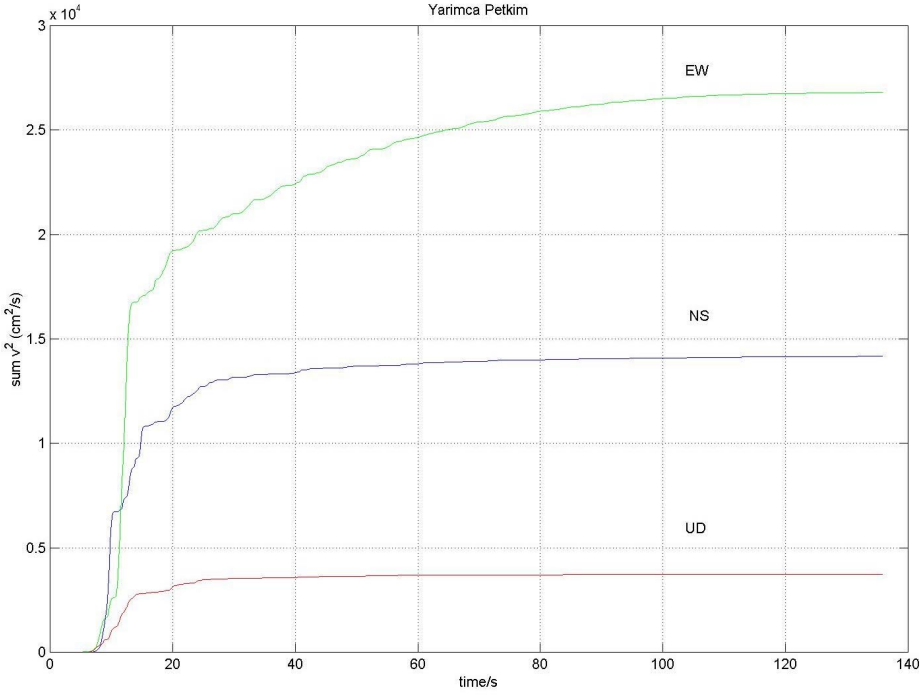
Yarimca Petkim
x 10^4
EW
NS
UD
sum v^2 (cm^2/s)
time/s

(a)

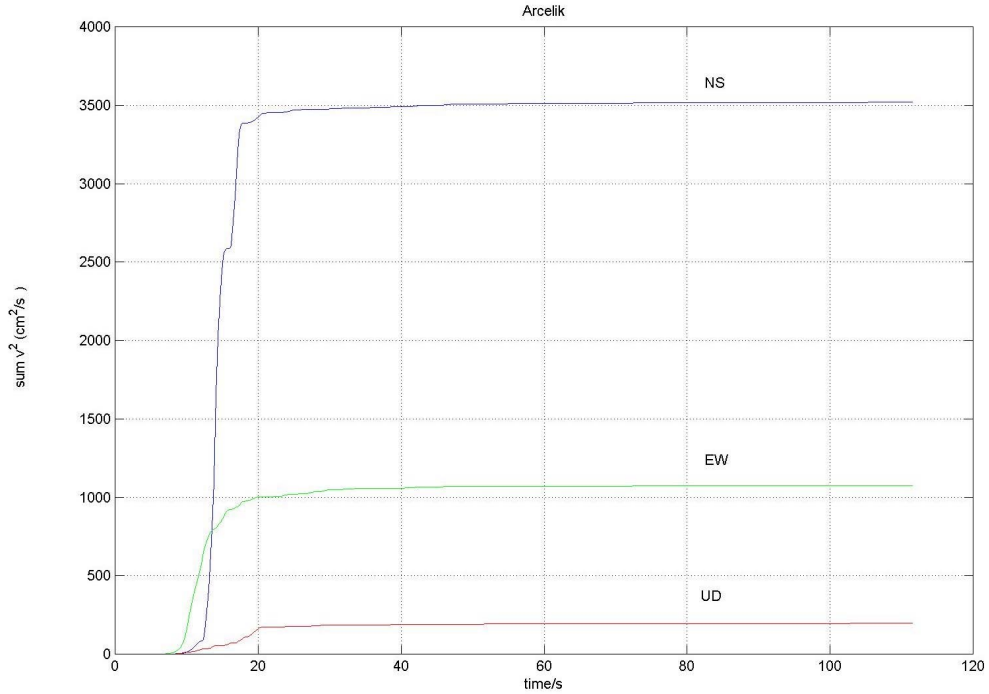
Arcelik
NS
EW
UD
sum v^2 (cm^2/s)
time/s

(b)

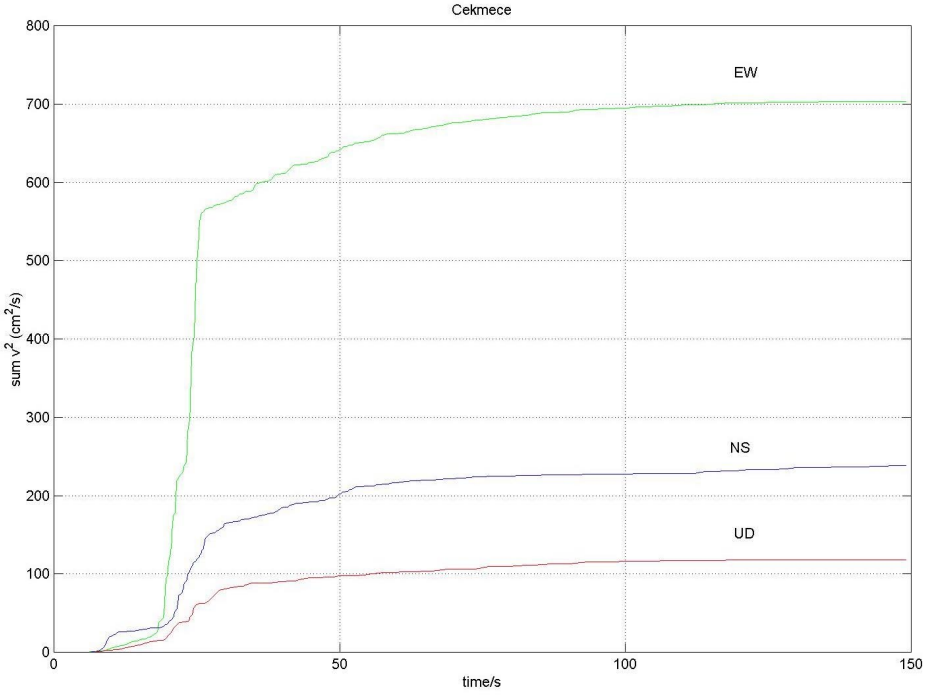

(c)

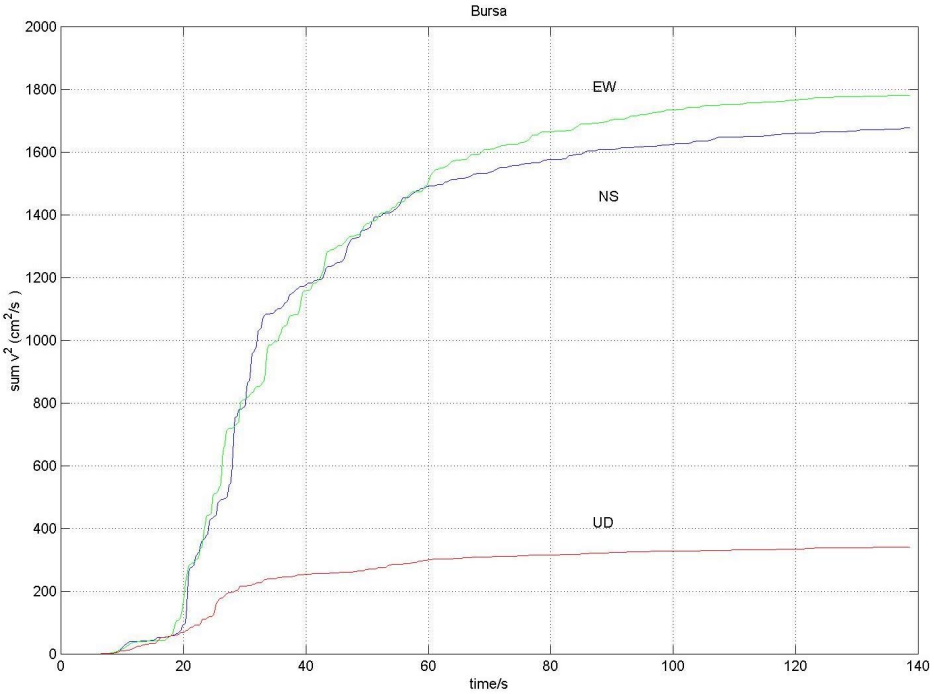

(d)

Figure 3.6.1 The relative cumulative significant shaking calculated by summing the square of velocity over time for a)YPT, b)ARC, c)CNA and d)BUR signals.

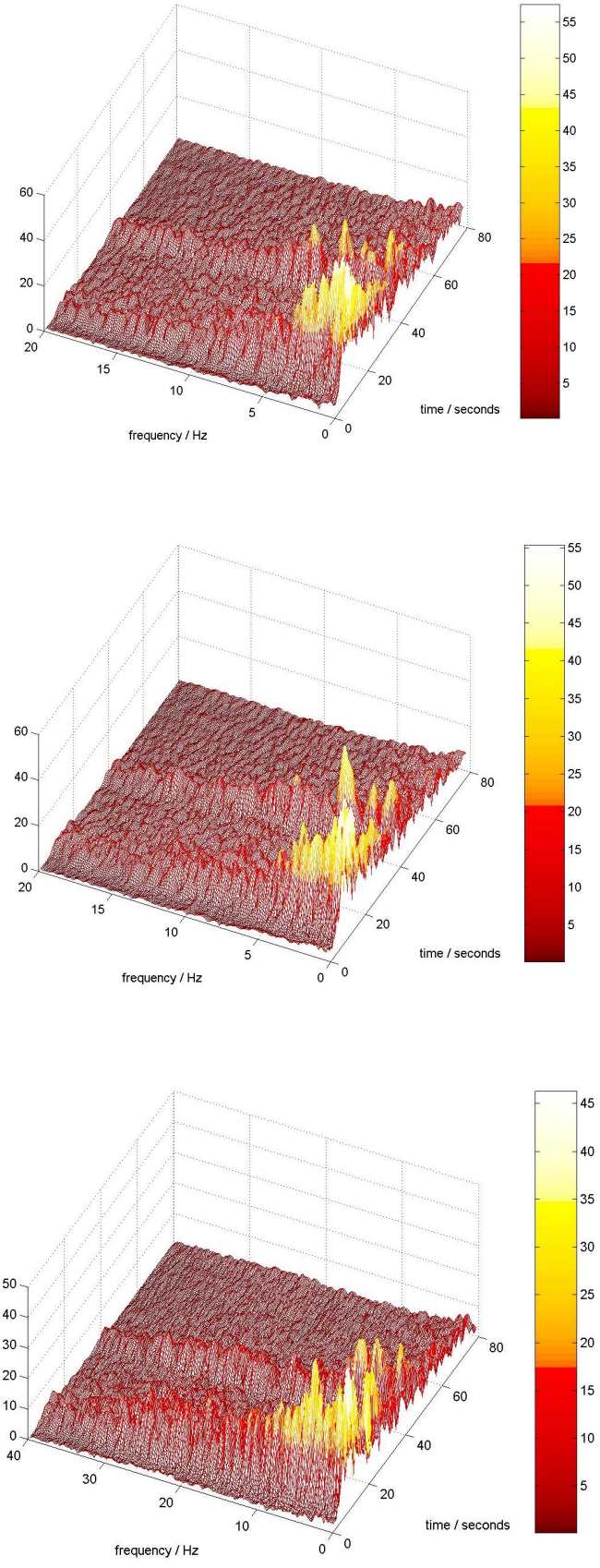

Figure 3.6.2a Mesh plot of YPT NS, EW, and UD components.

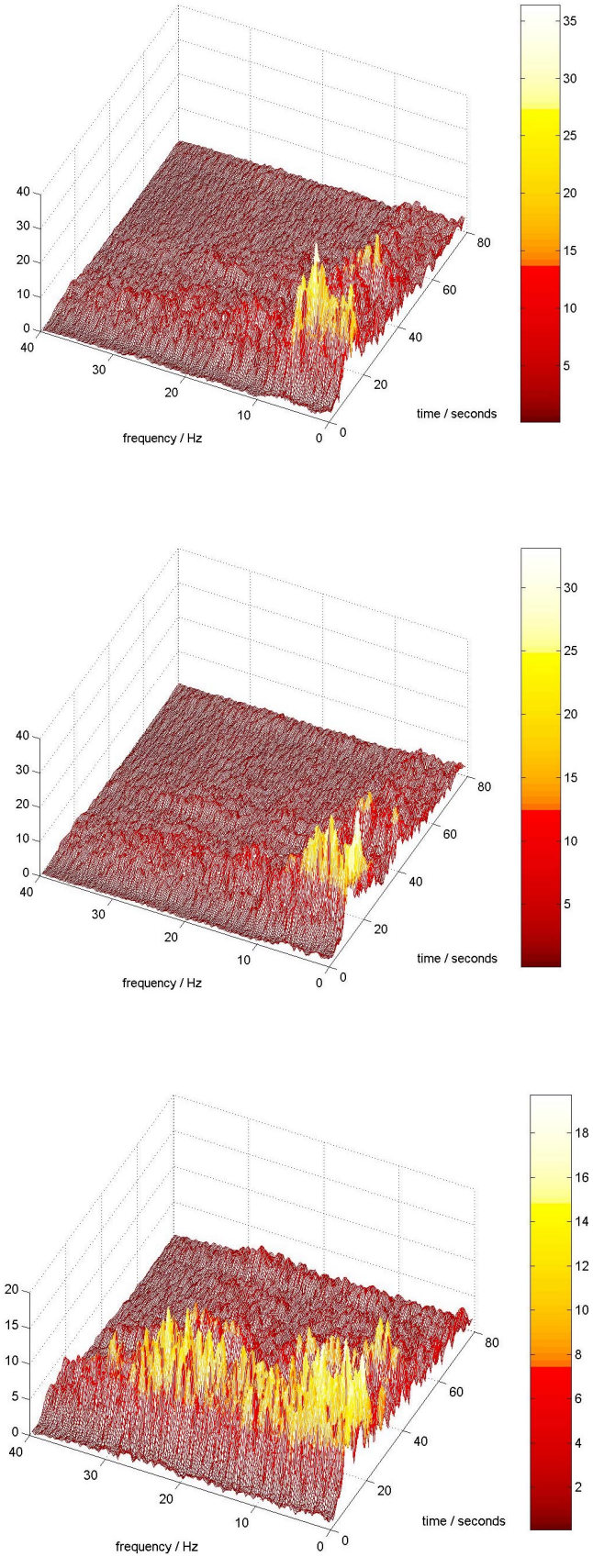

Figure 3.6.2b Mesh plot of ARC NS, EW, and UD components.

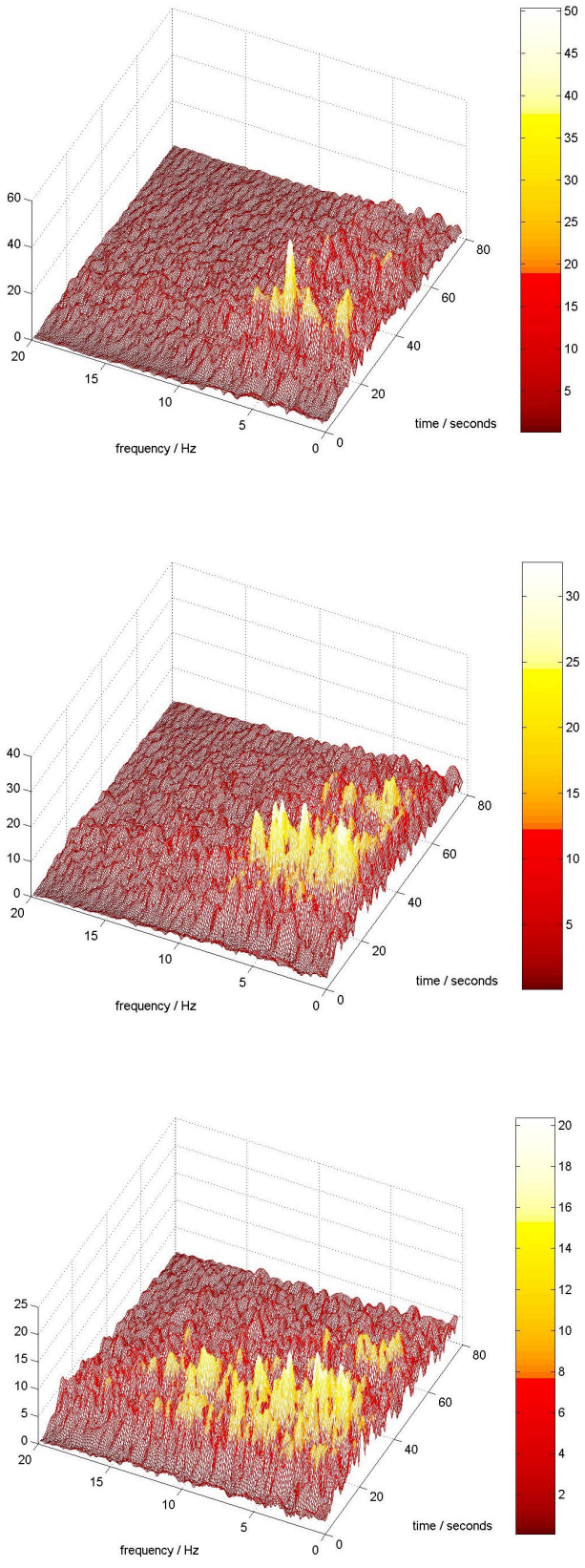

Figure 3.6.2c Mesh plot of CNA NS, EW, and UD components.

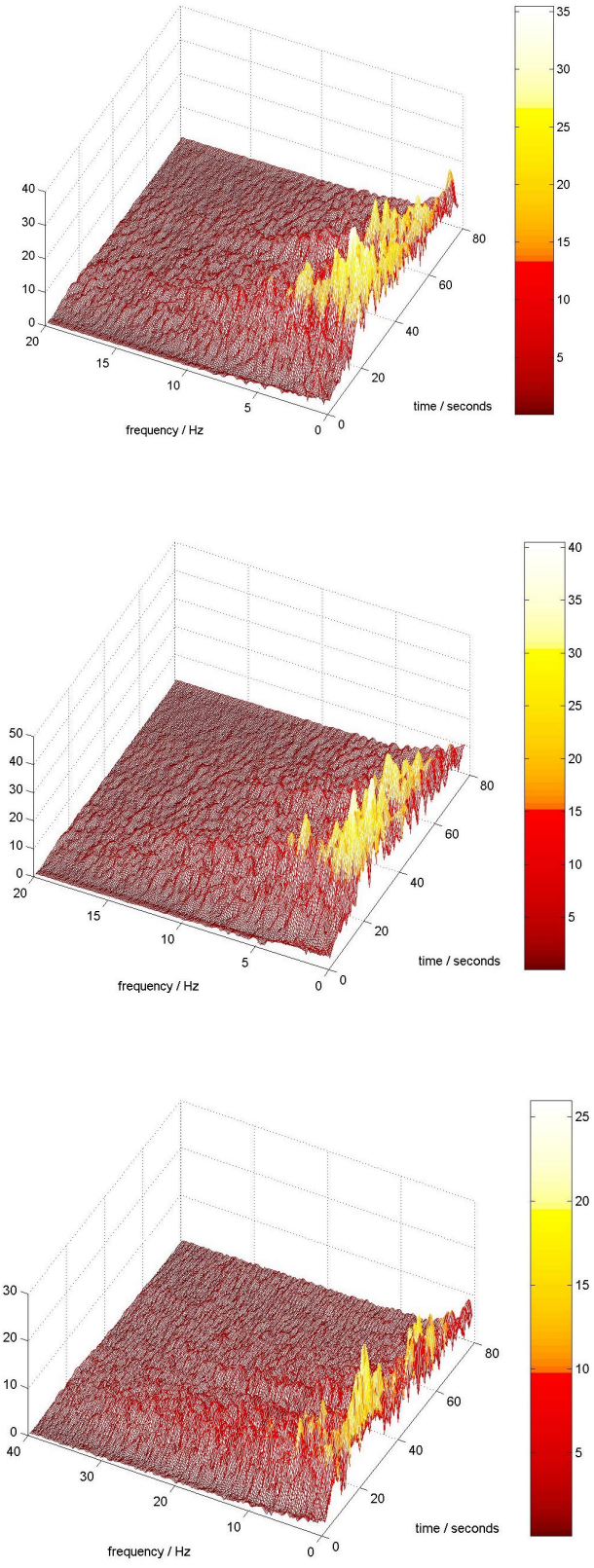

Figure 3.6.2d Mesh plot of BUR NS, EW, and UD components.

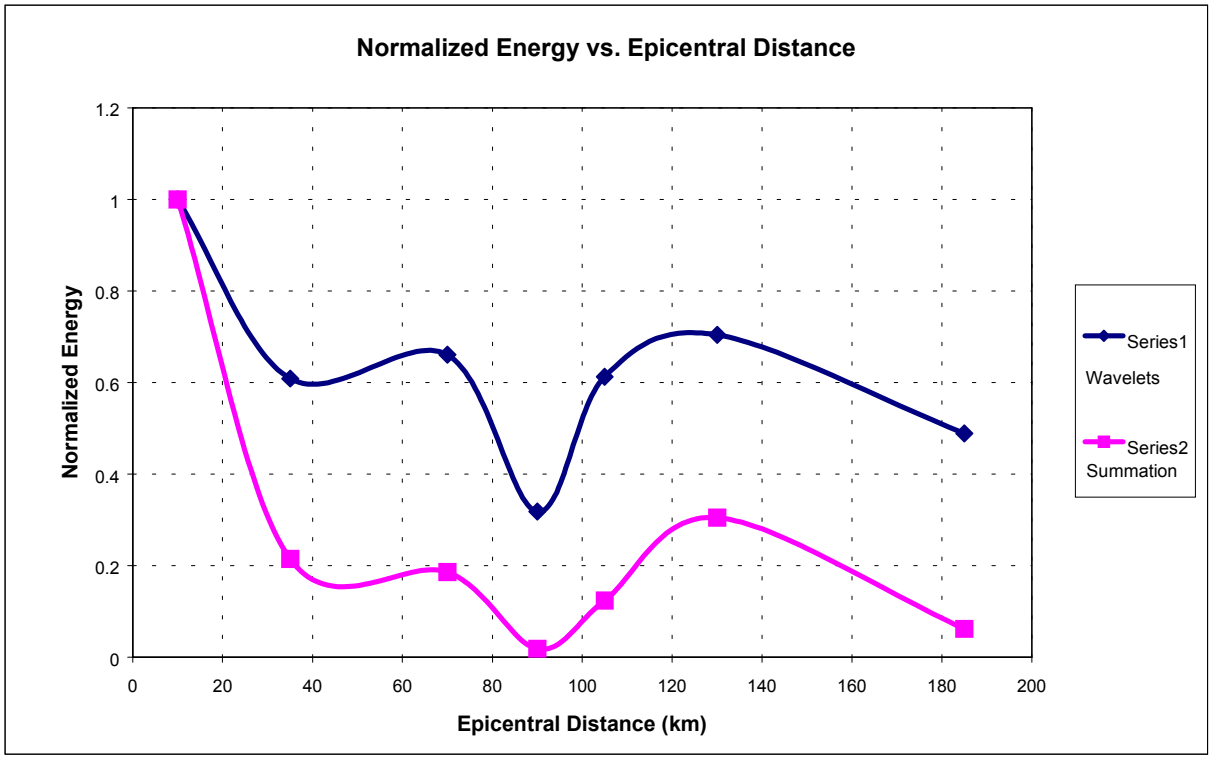

Figure 3.6.3 Normalised energy against epicentral distance.

3.7 Arias Intensity

To represent earthquakes delivering the same amounts of energy or having the same earthquake intensities, the Arias Intensity values were calculated. Arias Intensity index is the measure of the total energy which is delivered during an earthquake to a unit mass of soil. This is expressed following Arias (1970) as;

$$\mathrm{I} = \frac{\pi}{2g}\int_0^T a^2(t)dt \qquad (3.1)$$

where T is the total duration of the earthquake and a(t) is the acceleration at time, t.

Figure 3.7.1 shows the Arias intensity index against time, which is calculated by the above formula fro the four sites under consideration. Using the figures a comparison of energy distribution can be made and it can be seen that each component has a different intensity. These results are in agreement with the energies calculated by the previous method in section 3.6. However for the CNA signal they seem to differ, the

reason is unknown. As seen in Figure 3.7.1c two steps can be seen, one is the main shock and the other step represents the second rupture. This can be seen in 7.7.1b,c, and d, but not as clear as in 3.7.1a.

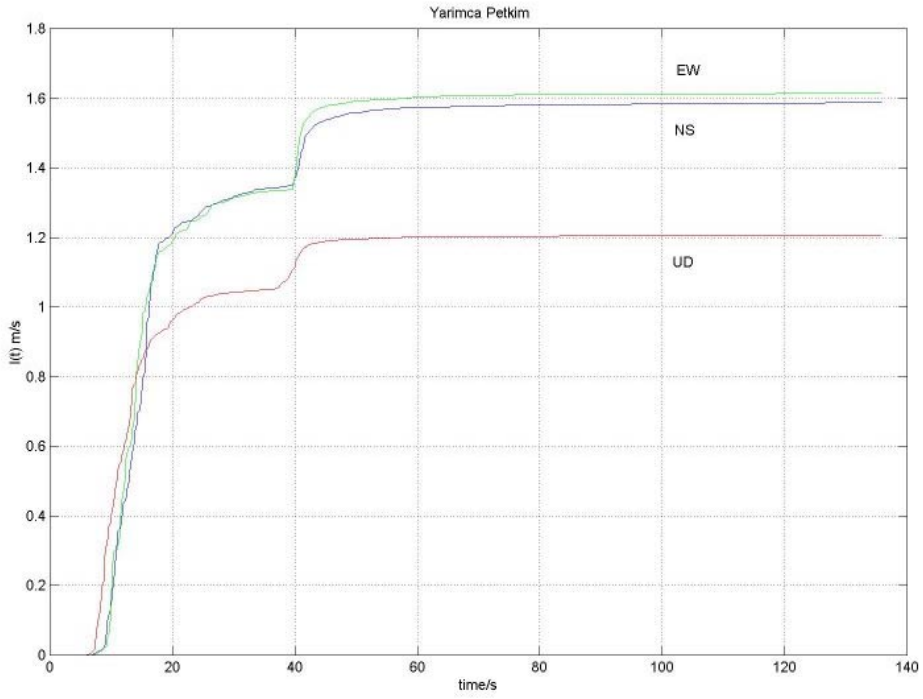

(a)

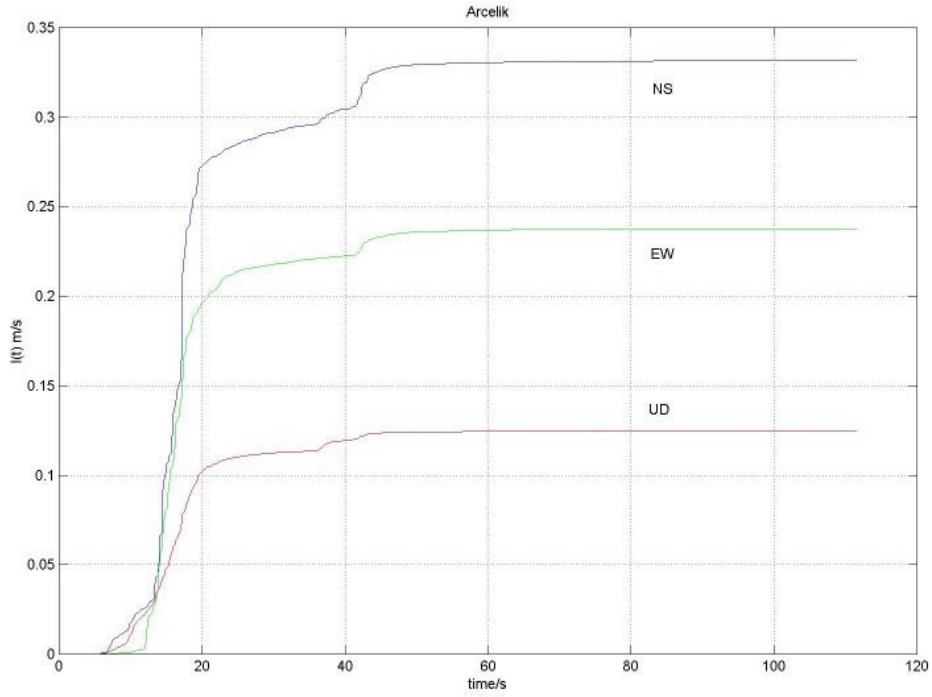

(b)

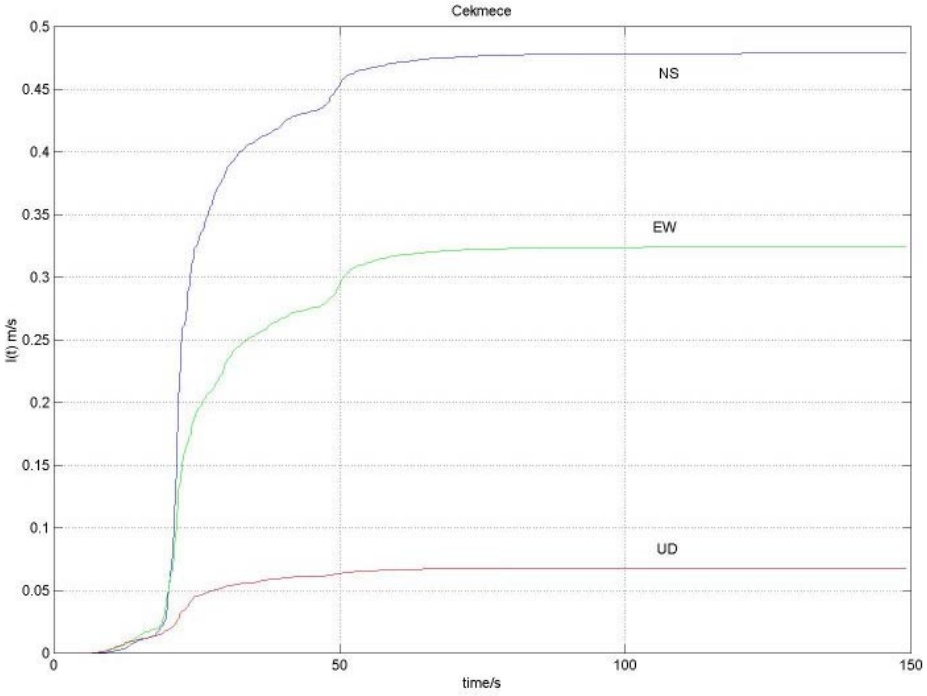

(c)

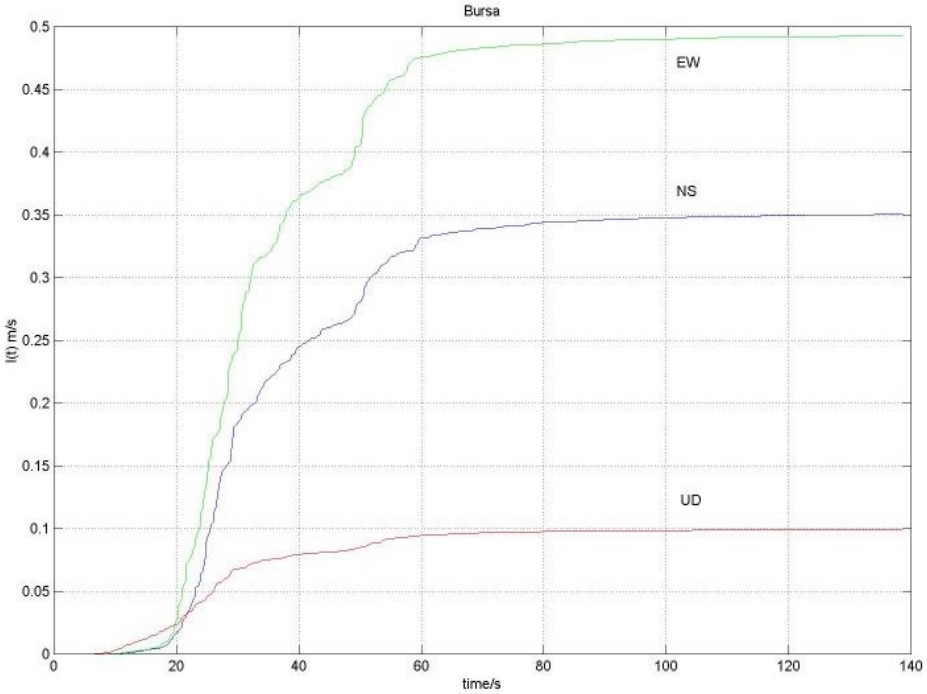

(d)

Figure 3.7.1 Arias Intensity graphs for a)YPT, b)ARC, c)CNA and d)BUR signals.

4. Conclusions

Velocities and displacements for this earthquake were calculated for the YPT station results as 70cm/s in NS, 70 cm/s in EW, and 40cm/s in the UD direction. The maximum displacements were 45cm, 80cm and 30cm in NS, EW, and UD directions respectively. (*http:/www.boun.edu.tr*) Even though the acceleration values were not high, the effective duration of the earthquake was about 35 seconds causing the damage to be intensified.

From the UD signals, arrival of P waves before S waves could be observed with peak accelerations occurring before the NS or EW component suggesting that vertical accelerations are caused by P waves and horizontal accelerations by S waves. The magnitude of accelerations decreases as one moves away from the epicentre. Wavelet transform allows us to see the discontinuities within the signal or the system and zoom in for closer inspection. Using the wavelets, it was observed that in the Kocaeli earthquake ground motions, acceleration with same frequency occurred at different time instants. This could not have been observed by standard DFFT methods.

In this technical report, four strong motion recording stations were looked at with increasing distances to the epicentre. Acceleration traces showed two significant peaks suggesting two distinct rupture events occurred. The observation of vibrations in UD direction before the main shock arrived in lateral directions suggest the arrival of P waves before S waves. Methods of analysis used in this report included the traditional FFT method and the new wavelet method. The results of the FFT analysis are that as one moves away from the epicentre, frequency content of the signals changes. The change of frequencies with epicentral distance could not be correlated as it is suspected that the local geology and the super-structure play an important part in the amplification of attenuation of different frequency components. With the wavelet analysis, the different time-frequency patterns which could not be seen with the traditional FFT analysis were observed. Most frequencies concentrated between 10-20 seconds of the earthquake for YPT and ARC and for CNA and BUR signals between 20-30 seconds.

Particle Acceleration Trajectories were used to observe the change of phase of the signals with time and distance to the epicentre. The phase change from 90° out of phase to 135° were observed in 15 seconds long time windows as time passed. Energy

of the signals were looked at by 3-D wavelet maps and summation of the velocity traces to see the total energy and spread of energy with time. 3D wavelet maps were used to compare the location of the peak accelerations. Total energy and spreading of the energy was observed with summation of acceleration traces and wavelet mesh maps respectively. The energy of the earthquake decreases, as it travels away from the epicentre. The contribution from different frequencies and times to the energy of the signal was achieved with wavelet analysis. The contour maps aided in the observation of the variation of the earthquake characteristics with time and frequency.

Reference:

1- Arias A., (1970), A Measure of Earthquake Intensity. In seismic design for nuclear power plants. Hansen, R.J. editor, MIT Press Cambridge, mass., pp.438-483.

2- Hlawatsch F., and Boudreaux-Bartels G.F. (1992), Linear and Quadratic Time-Frequency Signal Representations, IEEE Signal Processing Magazine, April 1992,pg.21-23.

3- Kocaeli Earthquake Report (2000), EEFIT (in preparation)

4- Newland D.E. (1993), Random Vibrations, Spectral and Wavelet Analysis, pp. 295-370.

5- Newland D.E. (1995), Signal Analysis by the Wavelet Method, CUED/C-MECH/TR65, pp.11-12.

6- Newland D.E., (1998), Time-frequency and Time-scale Signal Analysis by Harmonic Wavelets, chapter 1 of the book *Signal Analysis and Prediction*, A. Procházka, J. Uhlír, P.J.W. Rayner and N.G. Kingsbury (eds.), Birkhäuser, Boston.

7- Newland D.E., (1999a), Harmonic Wavelets in Vibrations and Acoustics, Phil.Trans.R.Soc.Lond.A., Vol. 357, pp.2607-2625

8- Newland D.E., (1999b), Ridge and Phase Identification in the Frequency Analysis of Transient Signals by Harmonic Wavelets, *J. Vib. and Acoustics*, Trans. ASME, Vol. 121.